Electronic Supplementary Material (ESI) for Soft Matter.

Tuning coulombic interactions to stabilize nematic and smectic ionic liquid crystal phases in mixtures of charged soft ellipsoids and spheres

Giacomo Saielli*[a], Tommaso Margola[b], Katsuhiko Satoh*[c]

Electronic Supporting Information

System ρ^* = 0.447

q^* = 0.0

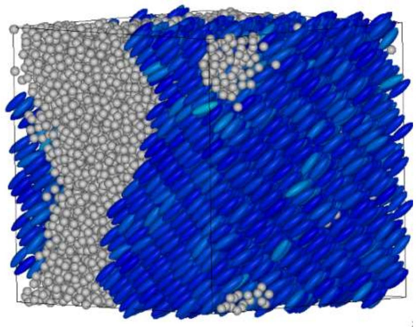

T* = 1.00

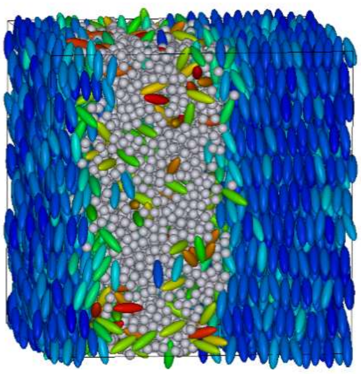

T* = 2.20

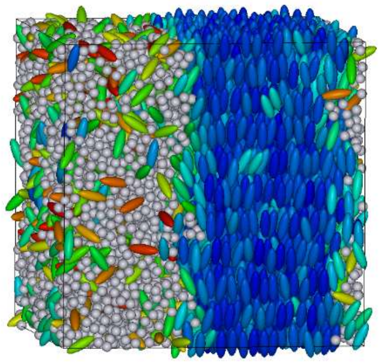

T* = 2.30

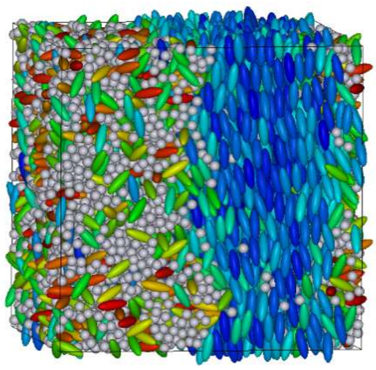

T* = 2.40

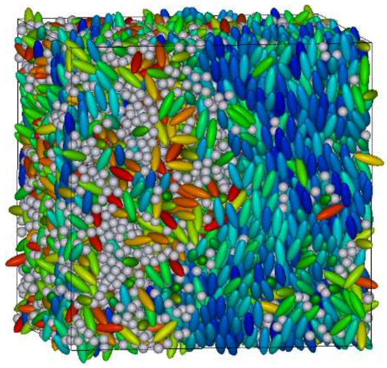

T* = 2.50

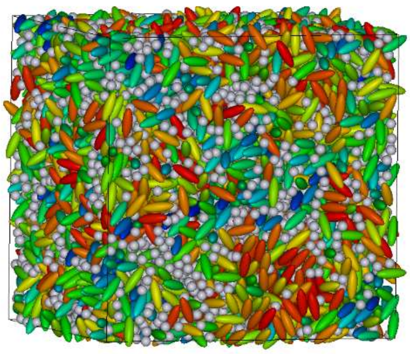

T* = 2.60

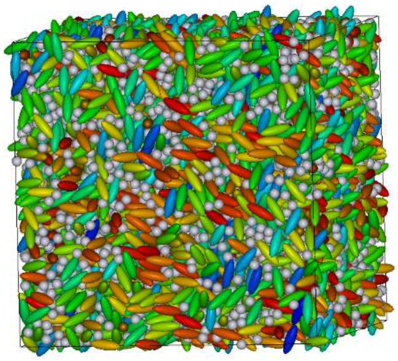

T* = 3.00

Figure S1. Snapshots obtained at the end of the production run for the system $\rho^* = 0.447$, $q^* = 0.0$.

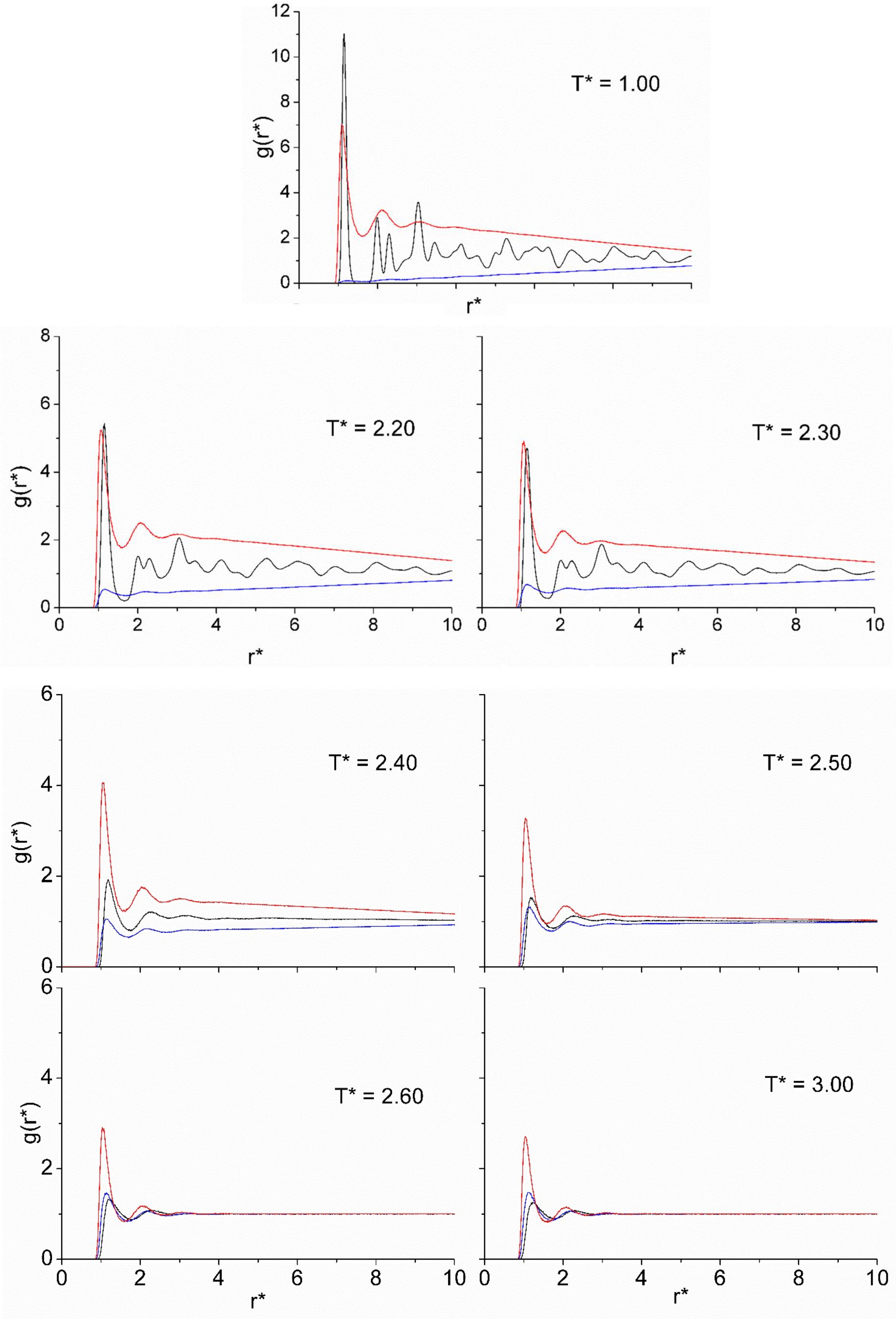

Figure S2. Radial distribution functions at the same temperatures of the snapshots of Figure S1 for the system ρ*= 0.447 and q* = 0.0. (black line) GB-GB RFD; (red line) LJ-LJ RDF; (blue line) GB-LJ RDF.

System ρ^* = 0.447

q^* = 0.5

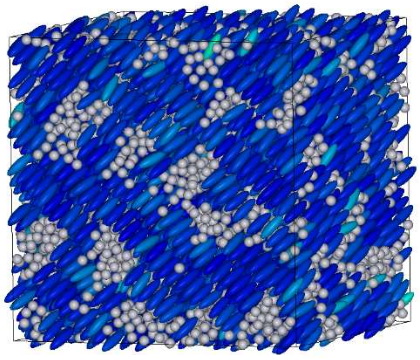

T* = 1.00

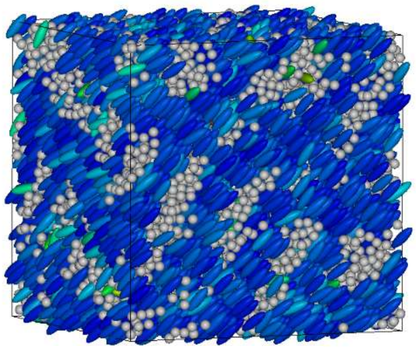

T* = 1.45

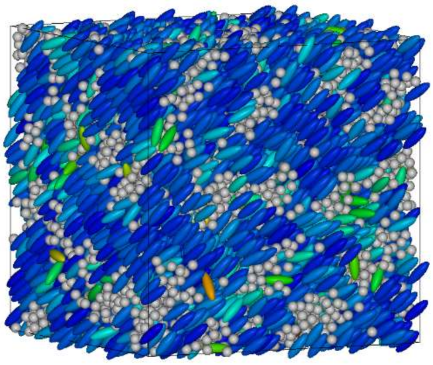

T* = 1.50

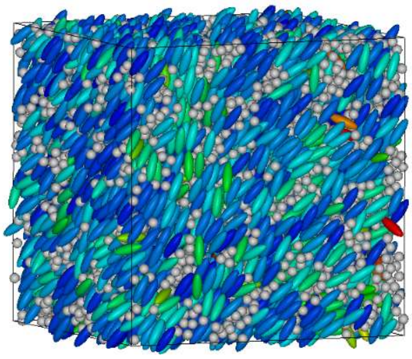

T* = 1.60

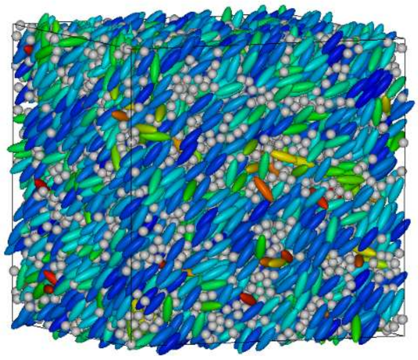

T* = 1.80

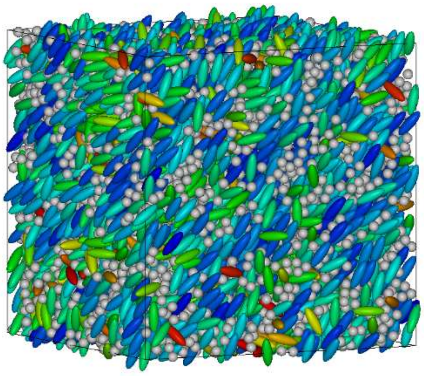

T* = 2.00

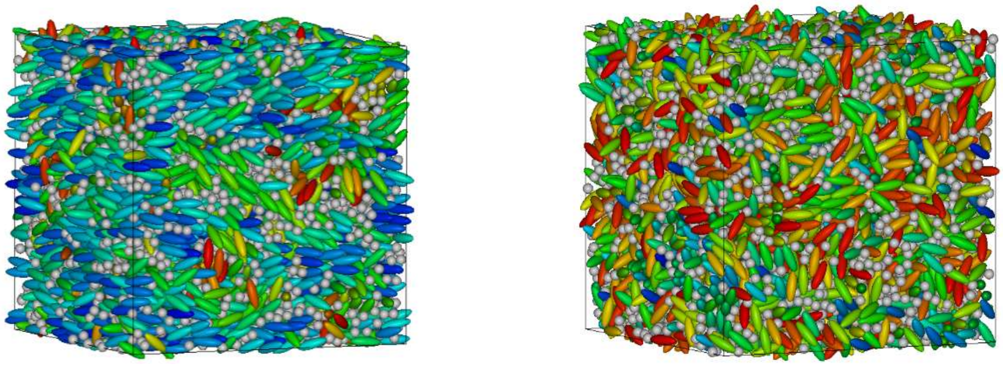

T* = 2.10 **T* = 2.50**

Figure S3. Snapshots obtained at the end of the production run for the system ρ^* = 0.447, q^* = 0.5

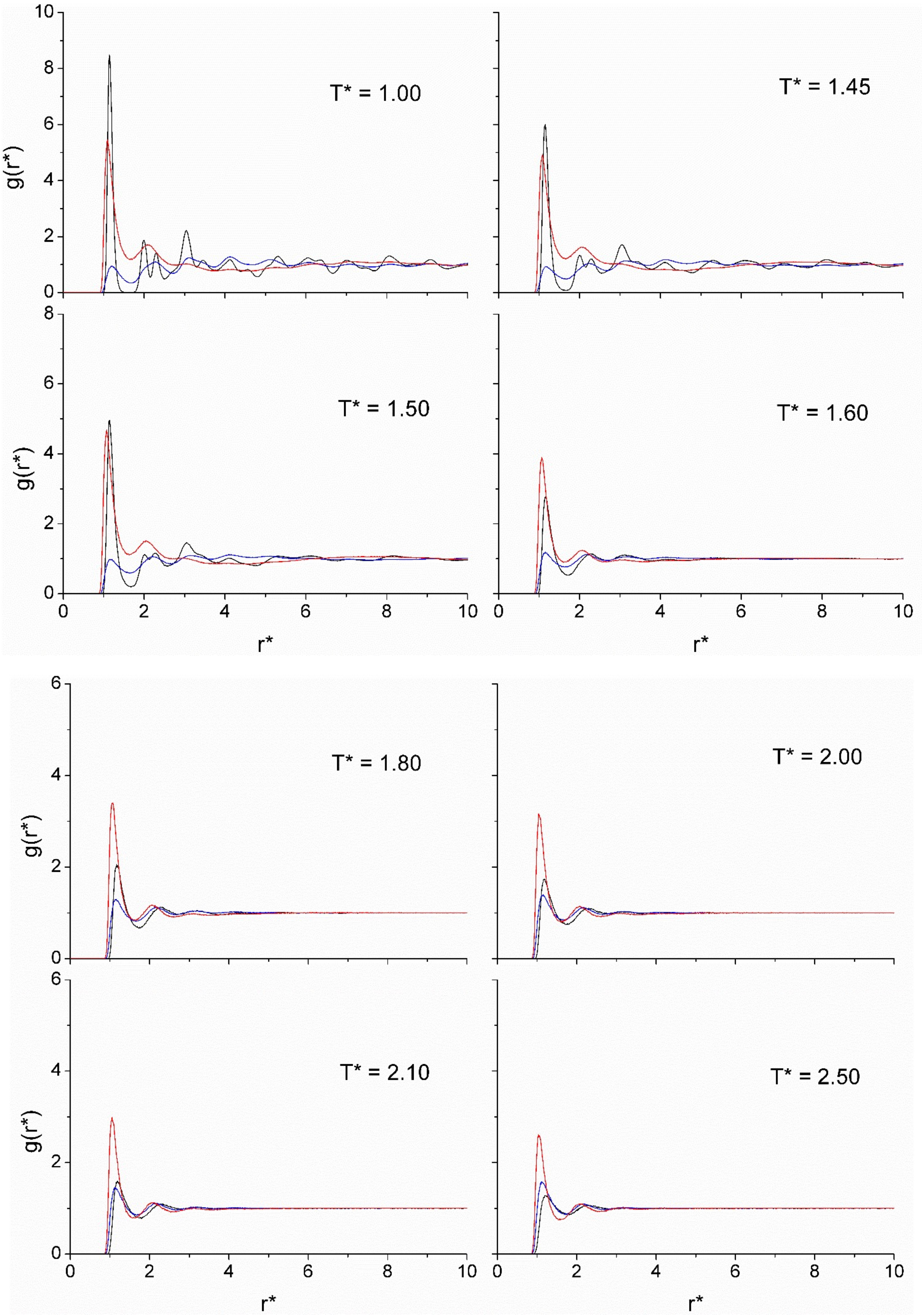

Figure S4. Radial distribution functions at the same temperatures of the snapshots of Figure S3 for the system ρ*= 0.447 and q* = 0.5. (black line) GB-GB RFD; (red line) LJ-LJ RDF; (blue line) GB-LJ RDF.

System ρ^* = 0.447

q^* = 2.0

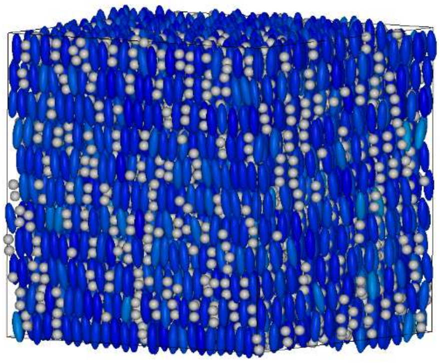

T* = 0.50

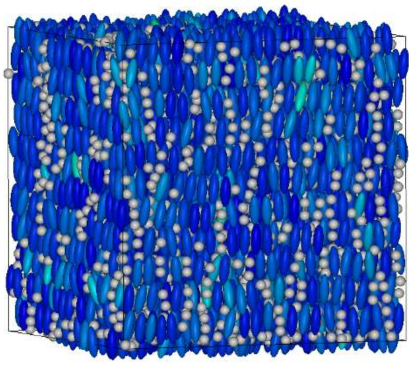

T* = 1.00

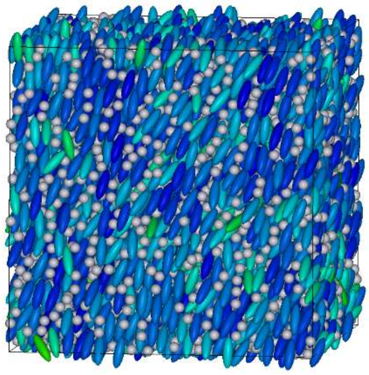

T* = 1.10

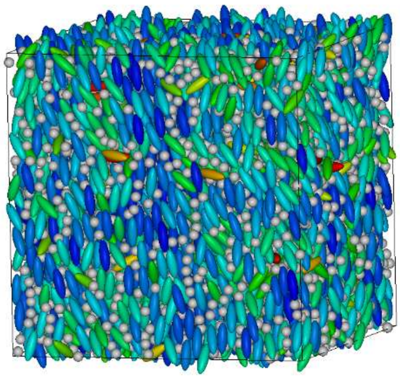

T* = 1.50

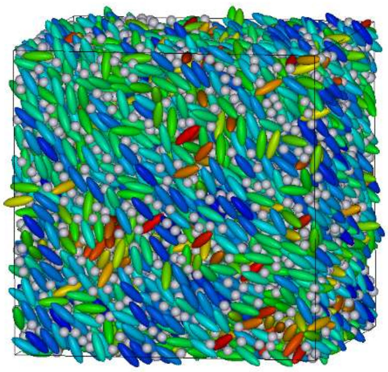

T* = 1.60

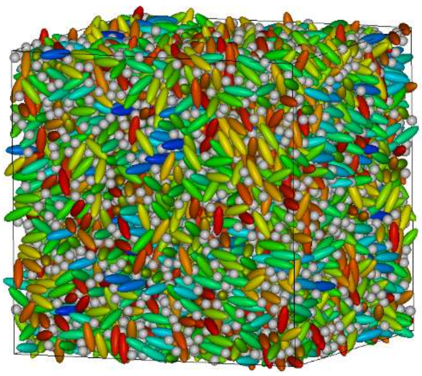

T* = 2.50

Figure S5. Snapshots obtained at the end of the production run for the system ρ^* = 0.447, q^* = 2.0

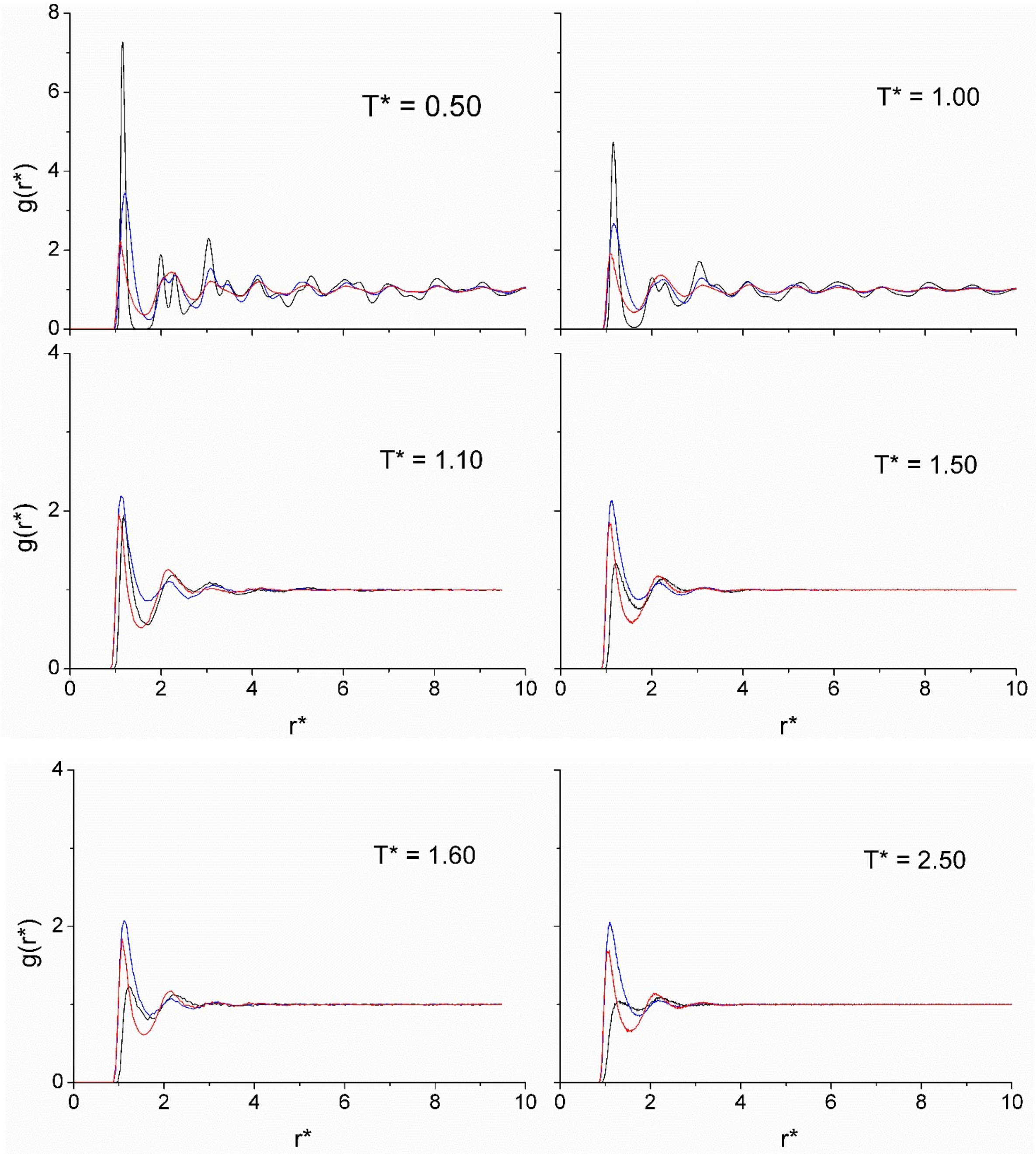

Figure S6. Radial distribution functions at the same temperatures of the snapshots of Figure S5 for the system ρ*= 0.447 and q* = 2.0. (black line) GB-GB RFD; (red line) LJ-LJ RDF; (blue line) GB-LJ RDF.

System ρ^* = 0.447

q^* = 5.0

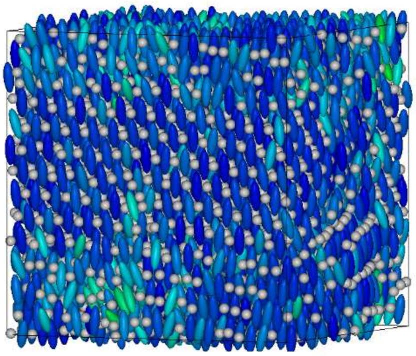

T* = 0.50

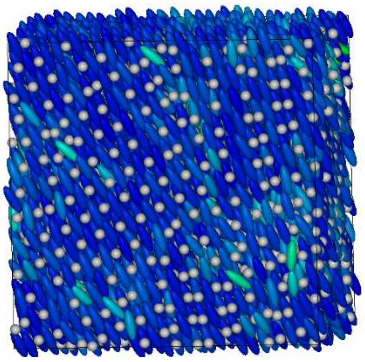

T* = 0.60

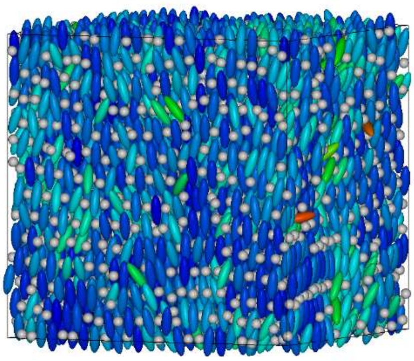

T* = 1.00

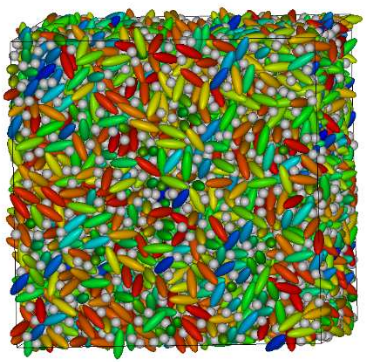

T* = 1.50

Figure S7. Snapshots obtained at the end of the production run for the system ρ^* = 0.447, q* = 5.0

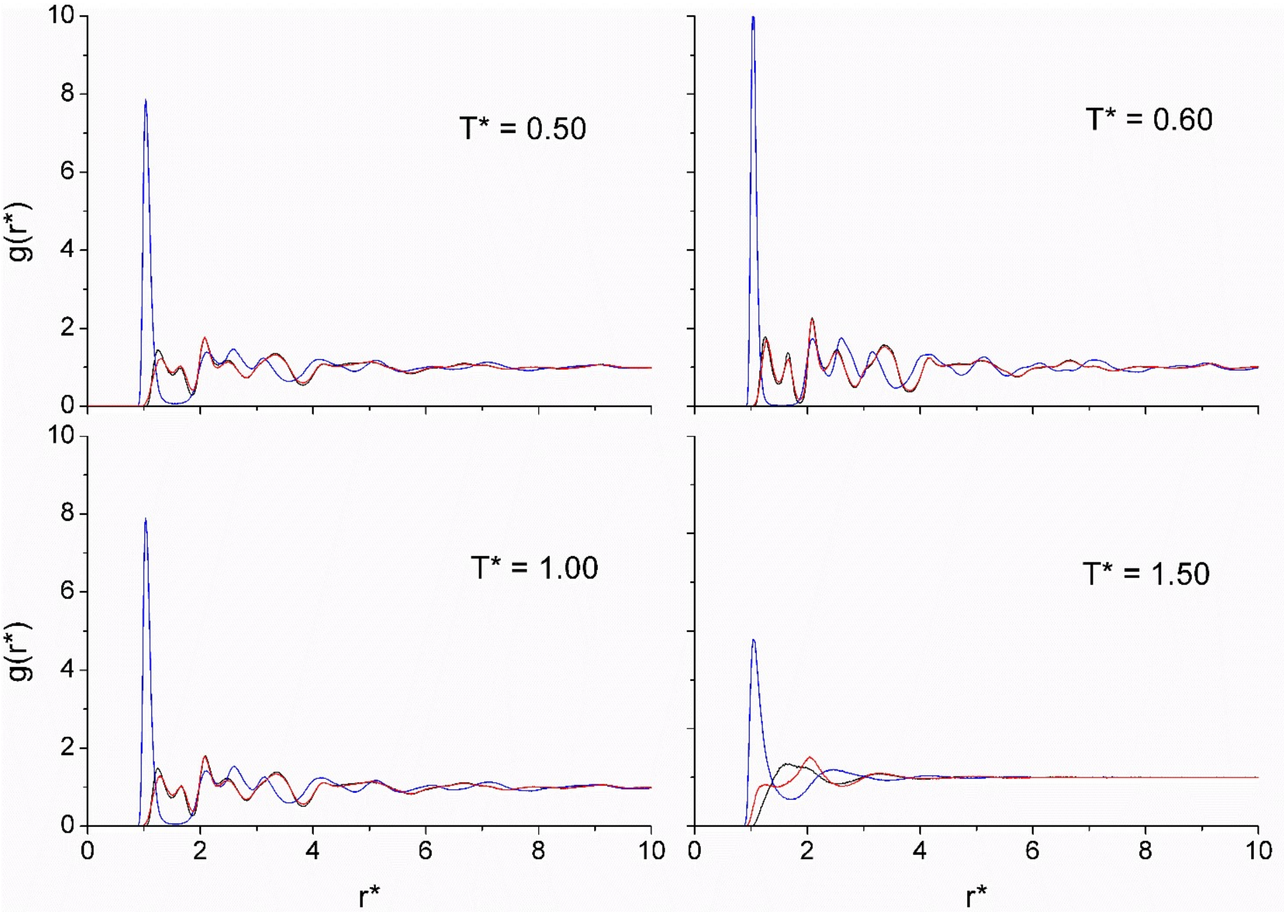

Figure S8. Radial distribution functions at the same temperatures of the snapshots of Figure S7 for the system ρ*= 0.447 and q* = 5.0. (black line) GB-GB RFD; (red line) LJ-LJ RDF; (blue line) GB-LJ RDF.

System ρ^* = 0.50

q^* = 0.0

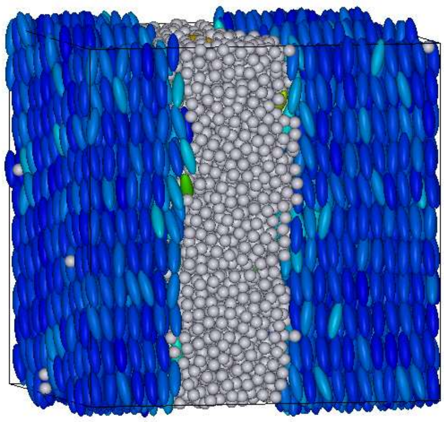

T* = 2.00

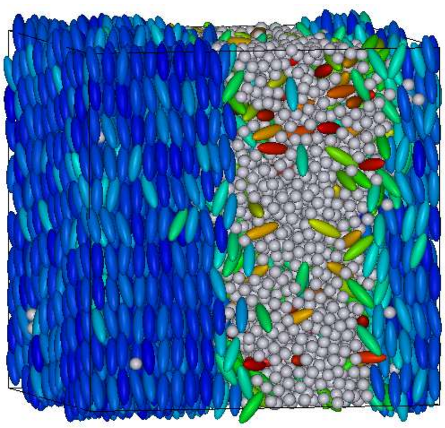

T* = 2.70

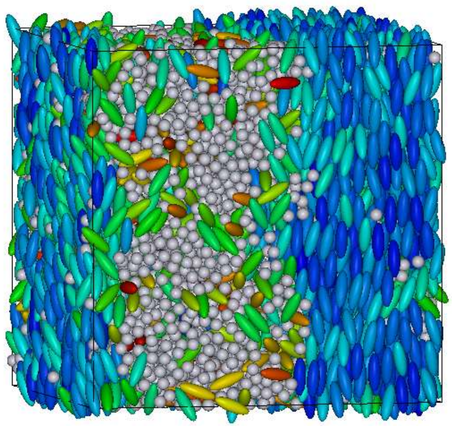

T* = 2.80

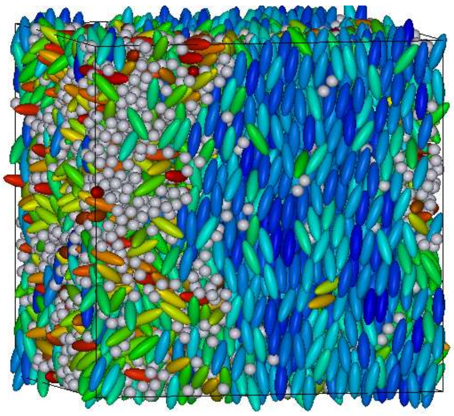

T* = 2.90

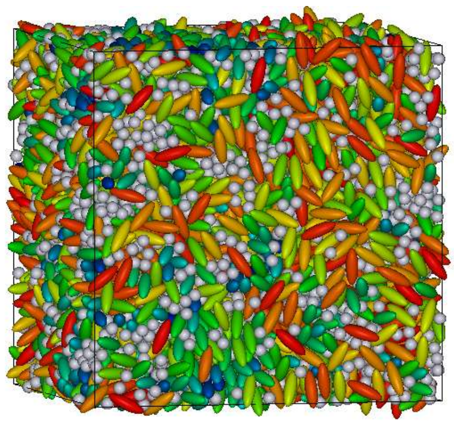

T* = 3.00

Figure S9. Snapshots obtained at the end of the production run for the system ρ^* = 0.50, q^* = 5.0

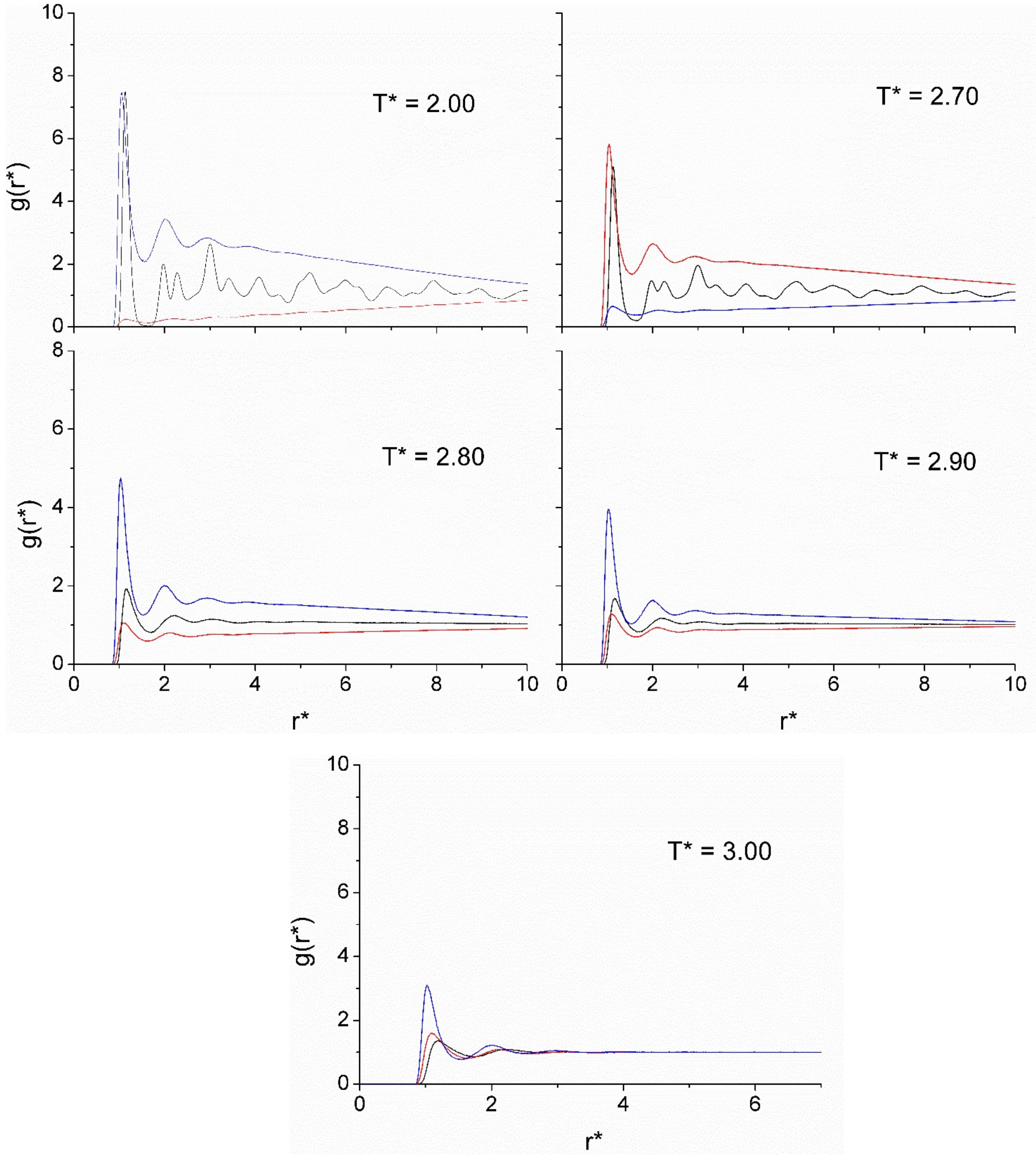

Figure S10. Radial distribution functions at the same temperatures of the snapshots of Figure S9 for the system ρ*= 0.50 and q* = 0.0. (black line) GB-GB RFD; (red line) LJ-LJ RDF; (blue line) GB-LJ RDF.

System ρ* = 0.50

*q** = 0.5

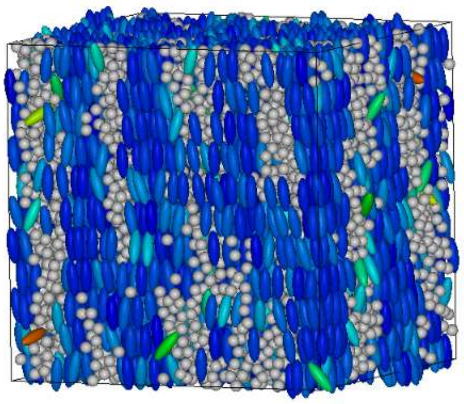

T* = 1.80

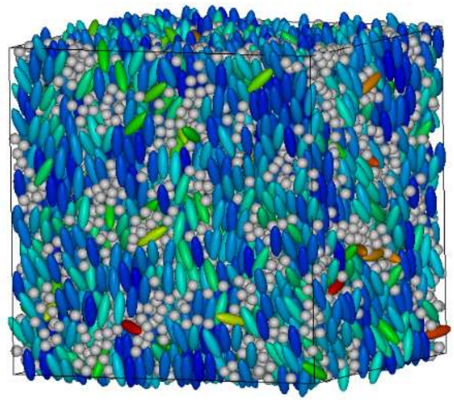

T* = 1.90

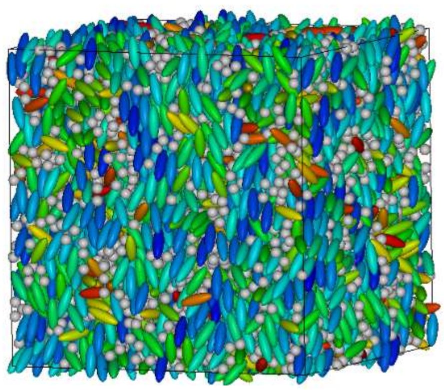

T* = 2.50

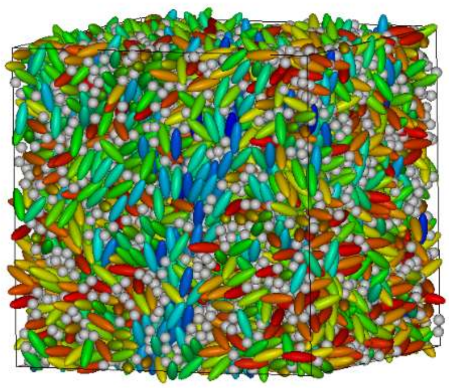

T* = 2.70

Figure S11. Snapshots obtained at the end of the production run for the system ρ* = 0.50, q* = 0.5

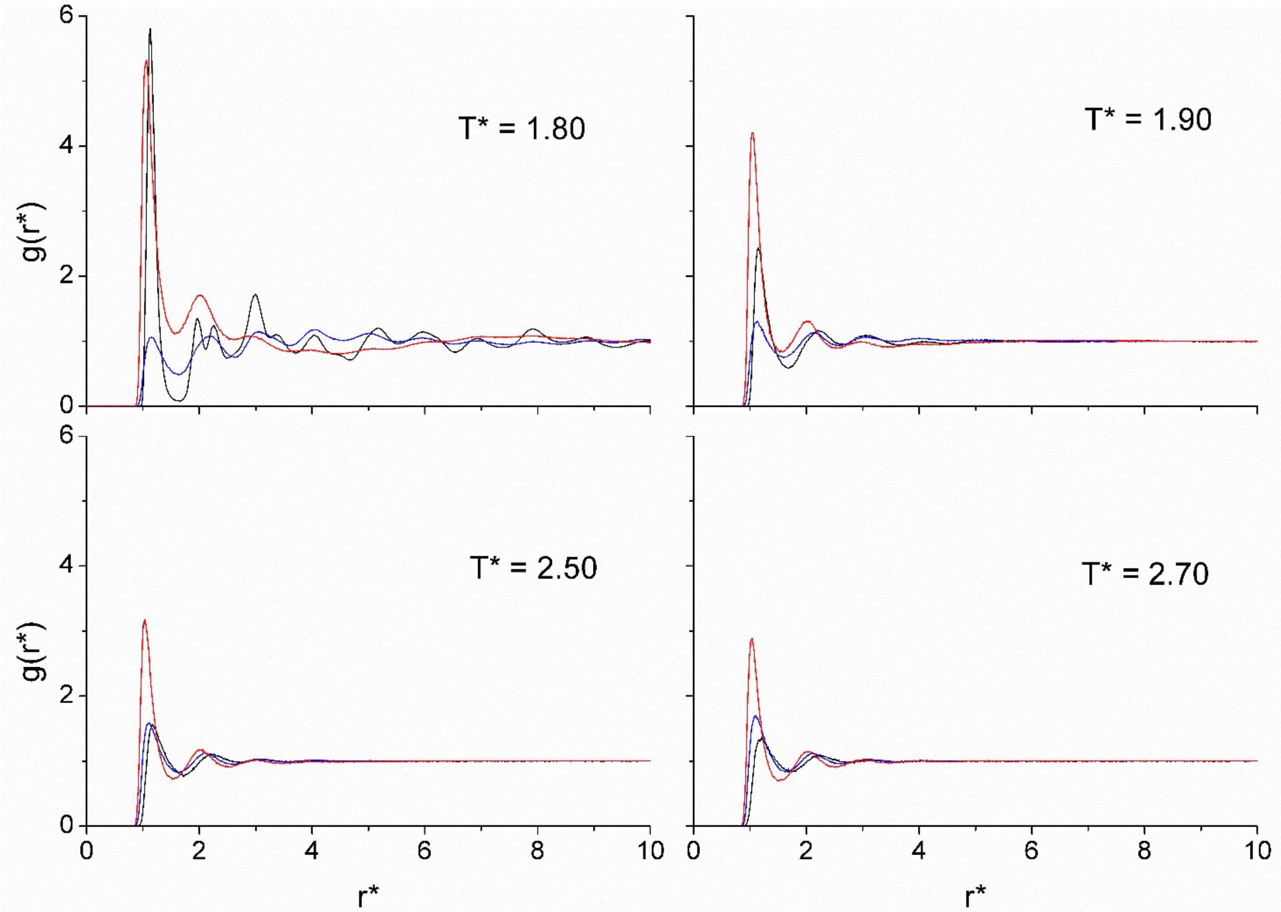

Figure S12. Radial distribution functions at the same temperatures of the snapshots of Figure S11 for the system ρ*= 0.50 and q* = 0.5. (black line) GB-GB RFD; (red line) LJ-LJ RDF; (blue line) GB-LJ RDF.

System ρ* = 0.50

*q** = 2.0

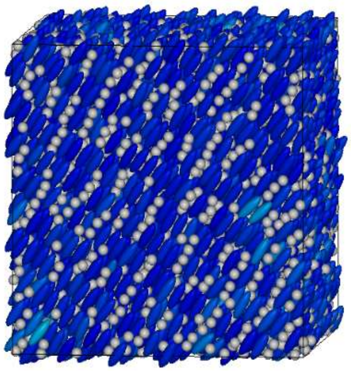

T* = 0.50

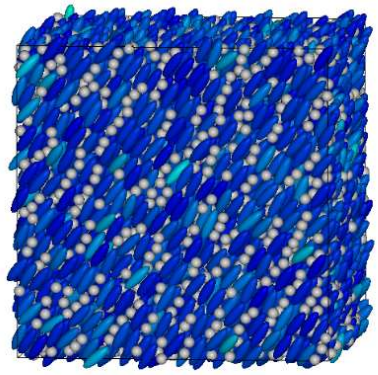

T* = 1.20

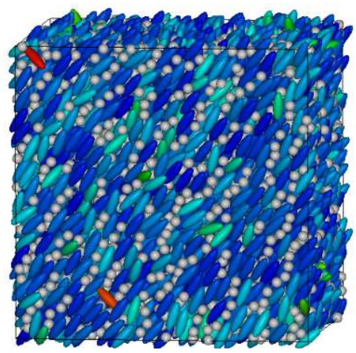

T* = 1.30

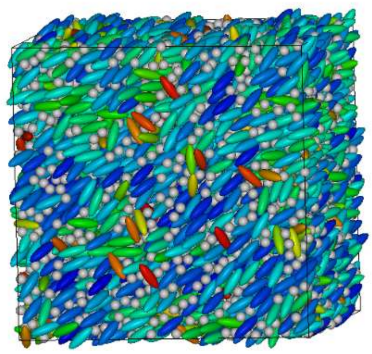

T* = 1.90

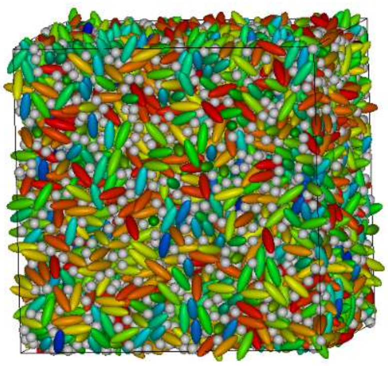

T* = 2.40

Figure S13. Snapshots obtained at the end of the production run for the system ρ* = 0.50, q* = 2.0

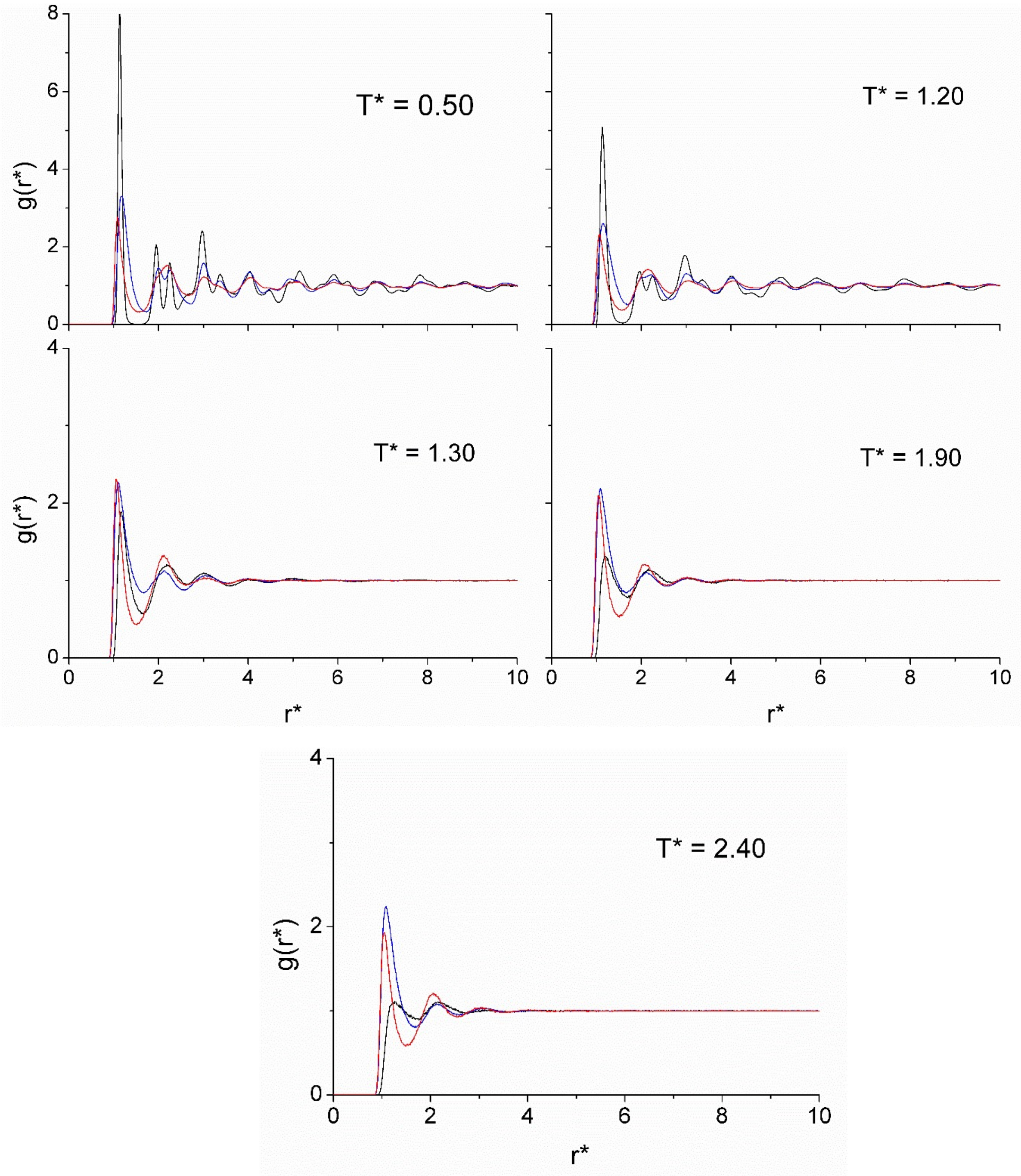

Figure S14. Radial distribution functions at the same temperatures of the snapshots of Figure S13 for the system ρ*= 0.50 and q* = 2.0. (black line) GB-GB RFD; (red line) LJ-LJ RDF; (blue line) GB-LJ RDF.

System ρ^* = 0.50

q^* = 5.0

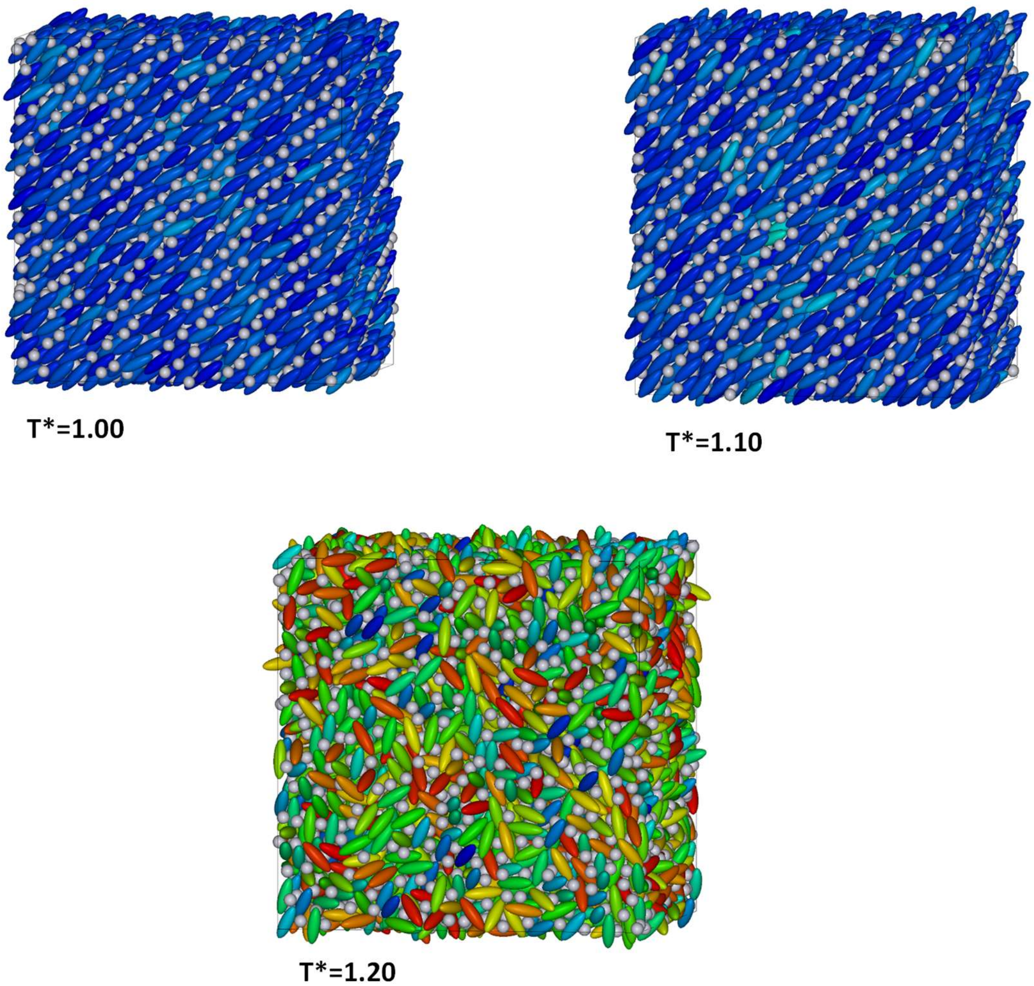

Figure S15. Snapshots obtained at the end of the production run for the system ρ^* = 0.50, q^* = 5.0

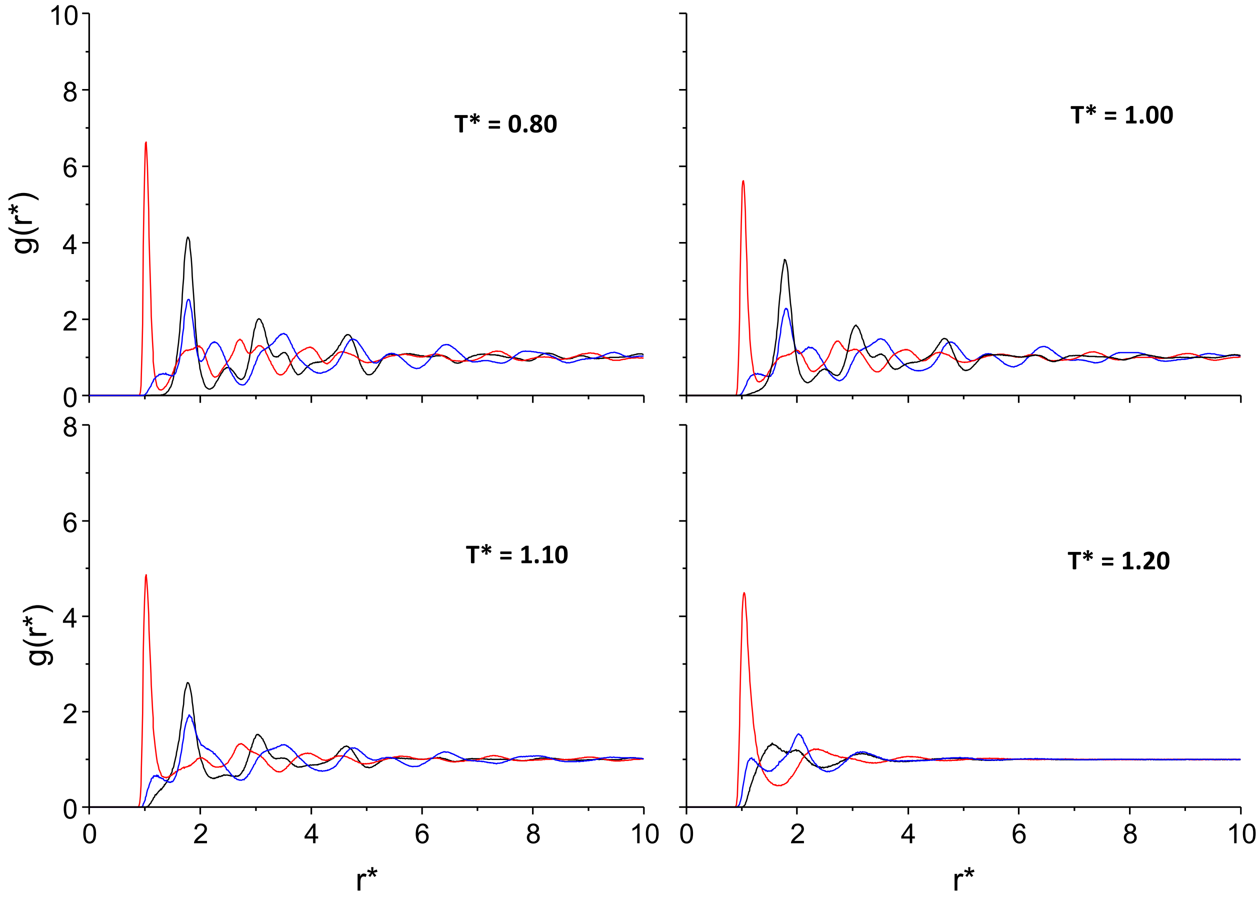

Figure S16. Radial distribution functions at the same temperatures of the snapshots of Figure S15 for the system ρ*= 0.50 and q* = 5.0. (black line) GB-GB RFD; (red line) LJ-LJ RDF; (blue line) GB-LJ RDF.

System ρ^* = 0.56

q^* = 0.0

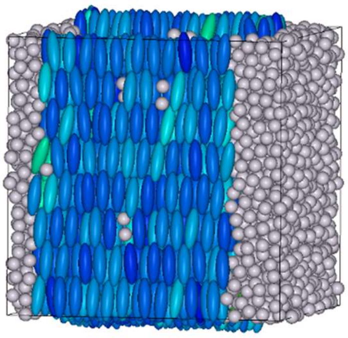

T*=2.0

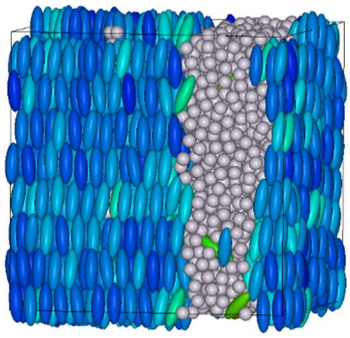

T*=2.4

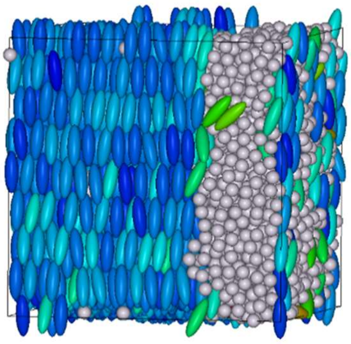

T*=2.6

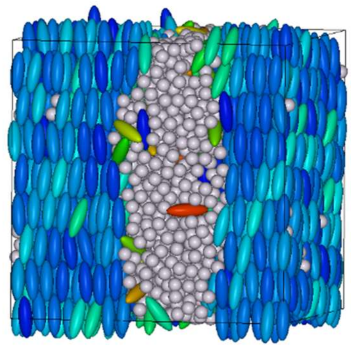

T*=2.8

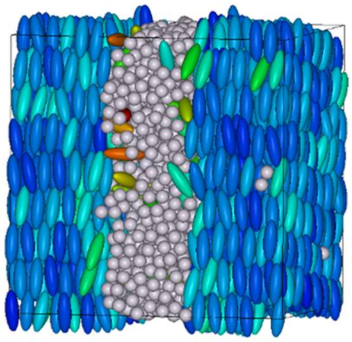

T*=3.0

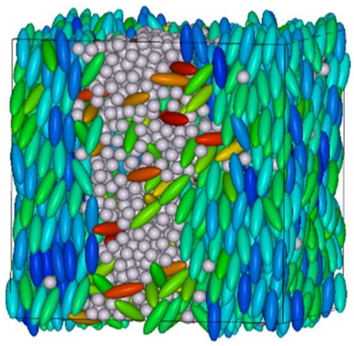

T*=3.1

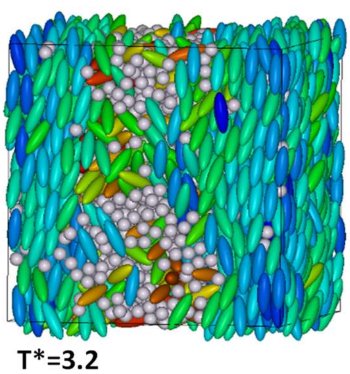

T*=3.2

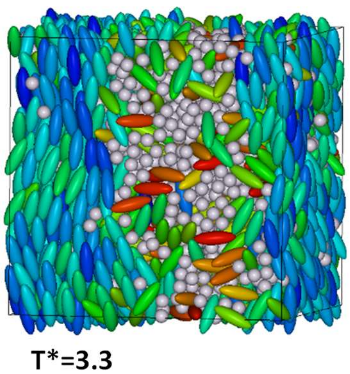

T*=3.3

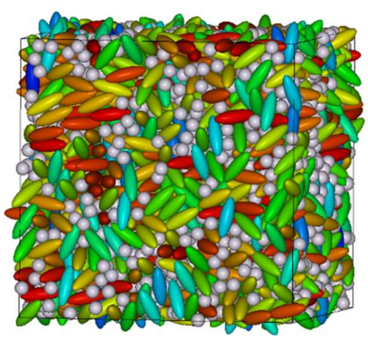

T*=3.4

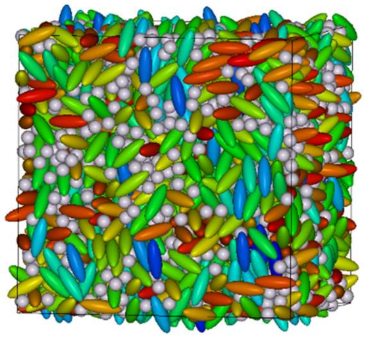

T*=3.5

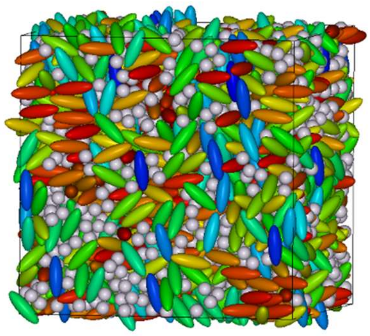

T*=3.8

Figure S17. Snapshots obtained at the end of the production run for the system ρ^* = 0.56, q^* = 0.0

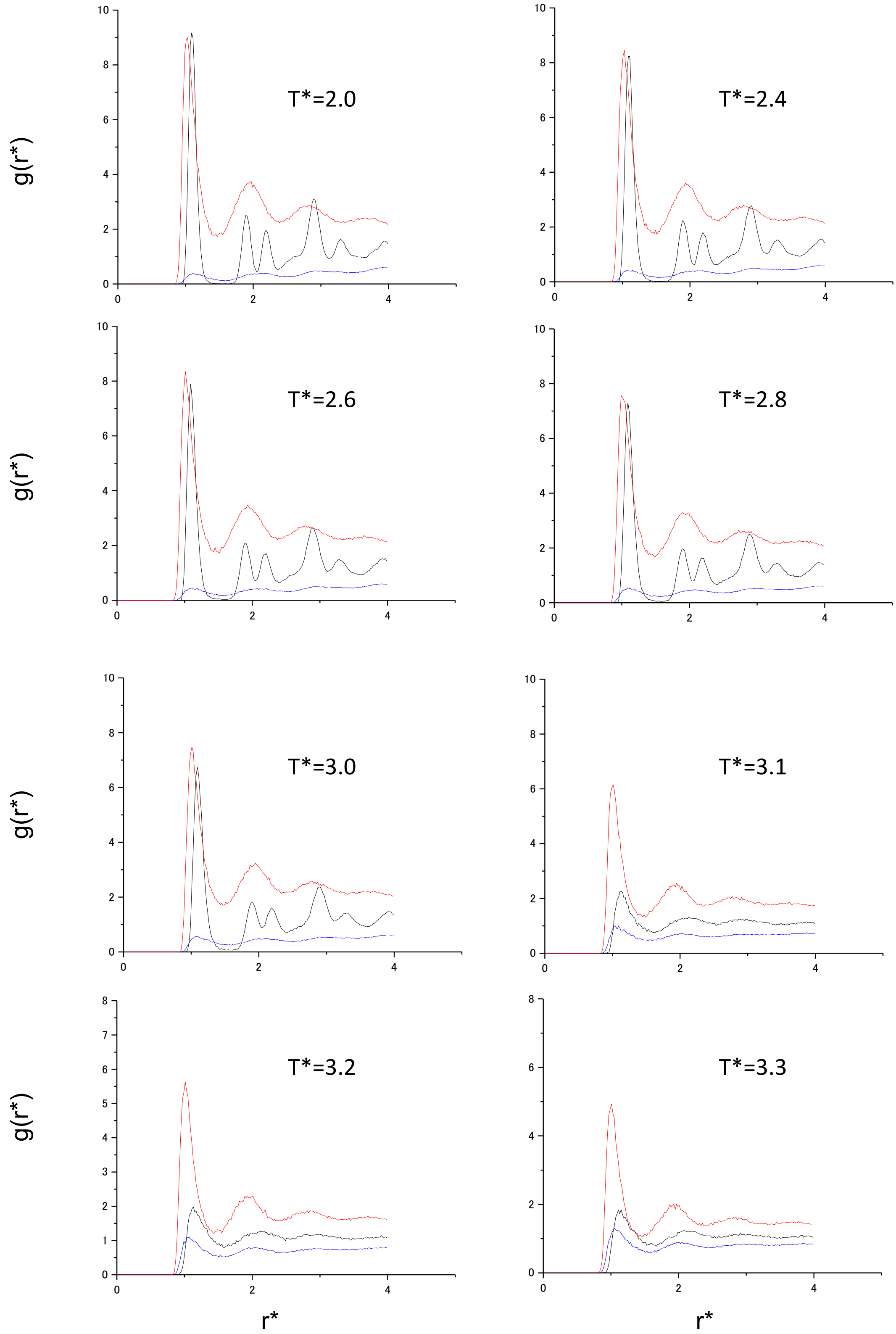
T*=2.0
T*=2.4
T*=2.6
T*=2.8
T*=3.0
T*=3.1
T*=3.2
T*=3.3
g(r*)
r*

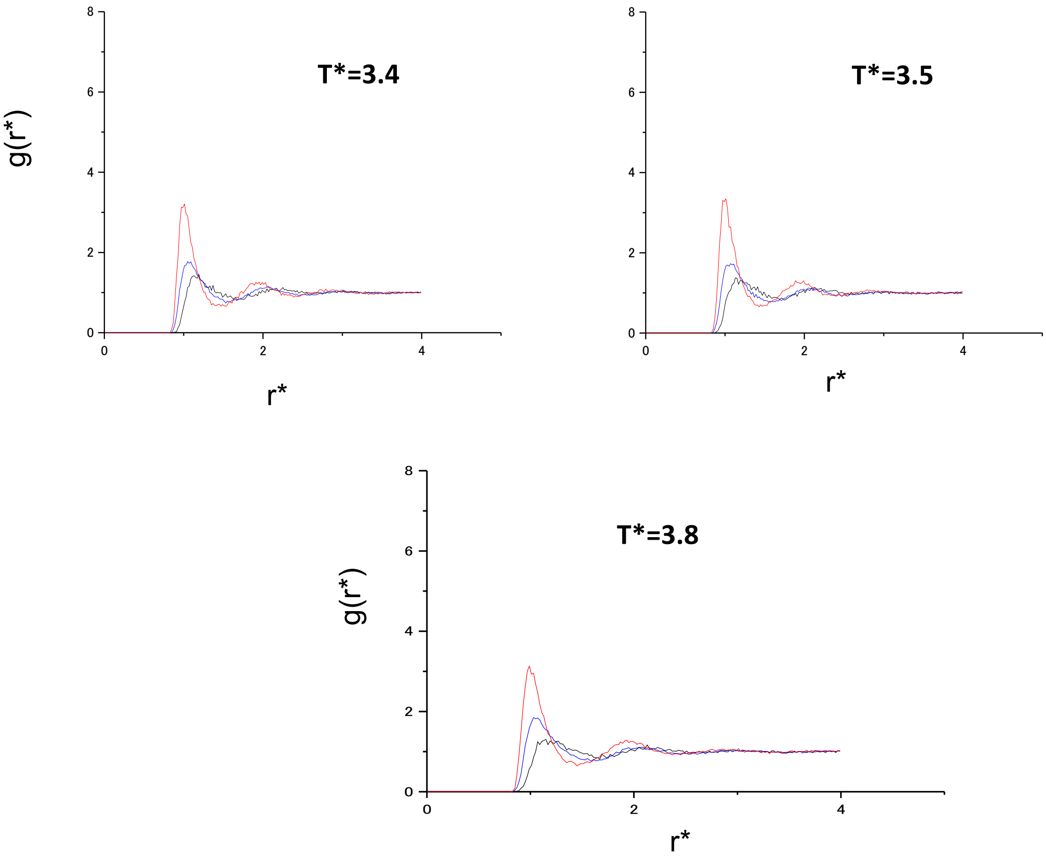

Figure S18. Radial distribution functions at the same temperatures of the snapshots of Figure S17 for the system ρ*= 0.56 and q* = 0.0. (black line) GB-GB RFD; (red line) LJ-LJ RDF; (blue line) GB-LJ RDF.

System ρ^* = 0.56

q^* = 0.5

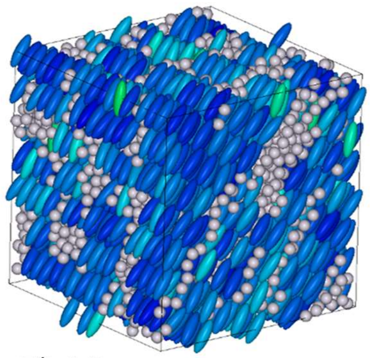

T*=1.8

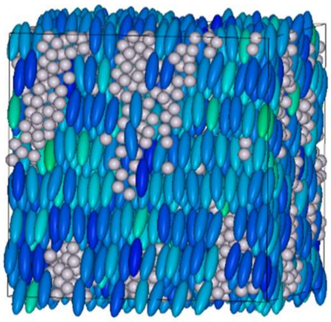

T*=1.9

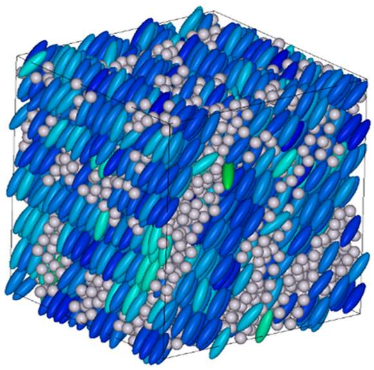

T*=2.0

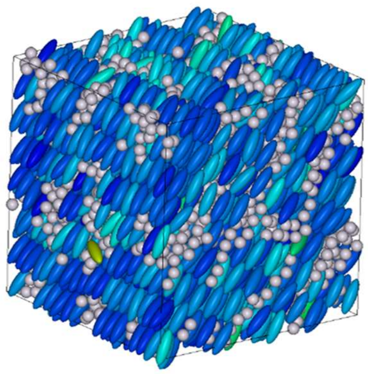

T*=2.1

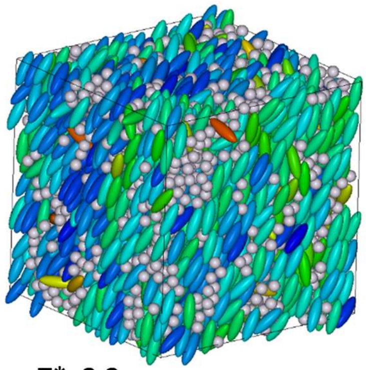

T*=2.2

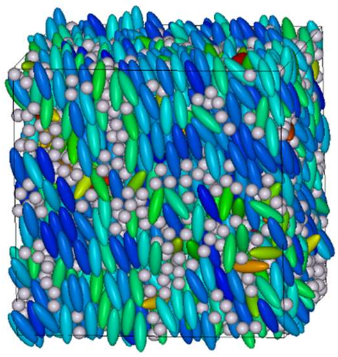

T*=2.5

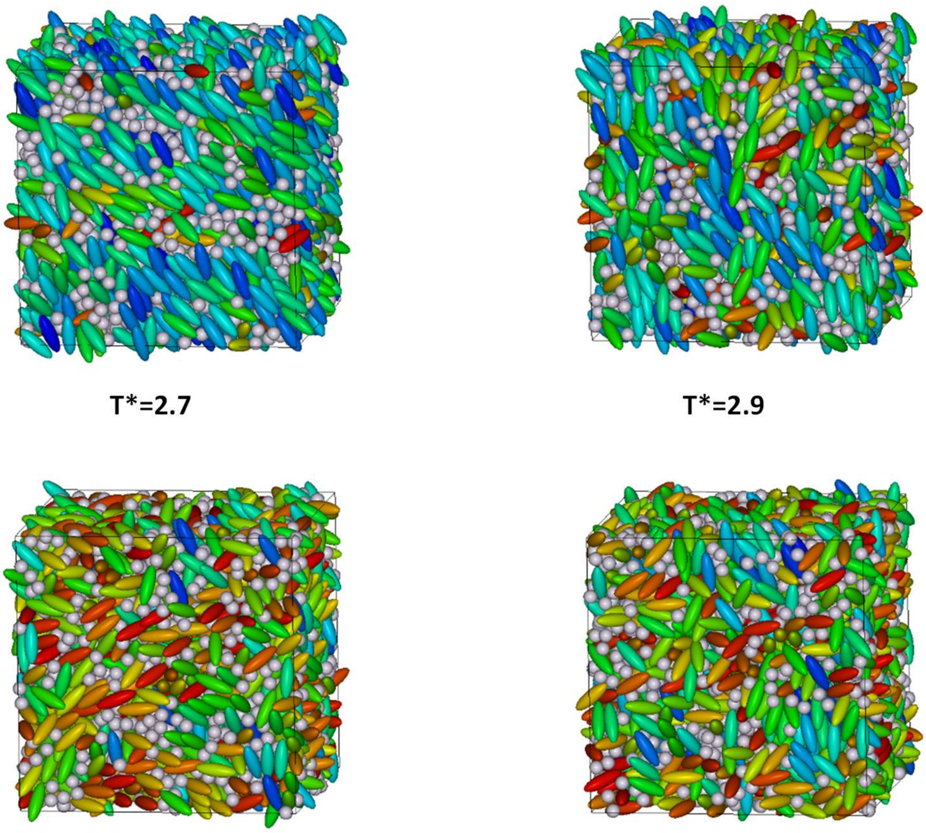

T*=2.7 T*=2.9

T*=3.0 T*=3.3

Figure S19. Snapshots obtained at the end of the production run for the system ρ* = 0.56, q* = 0.0

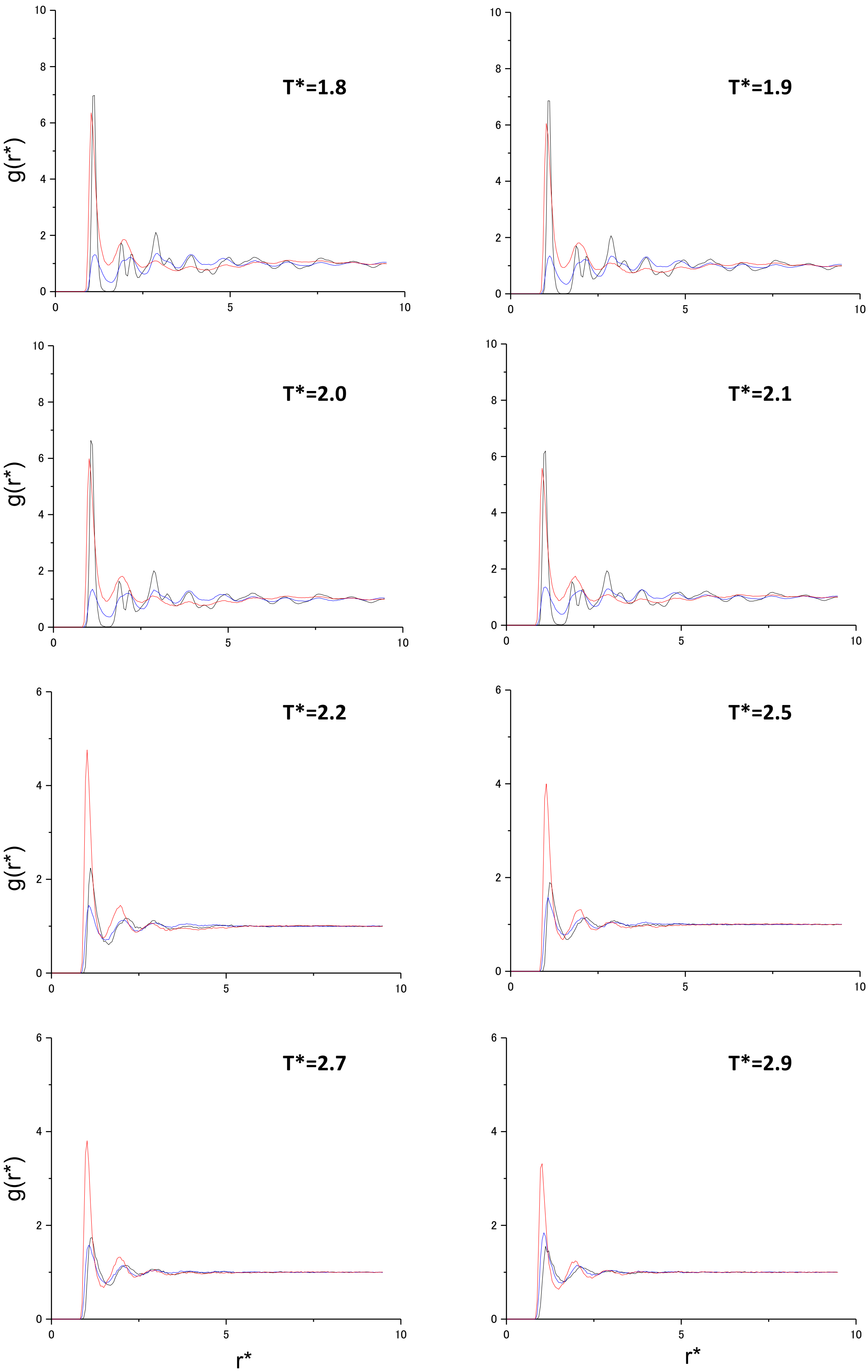
T*=1.8
T*=1.9
T*=2.0
T*=2.1
T*=2.2
T*=2.5
T*=2.7
T*=2.9
g(r*)
r*

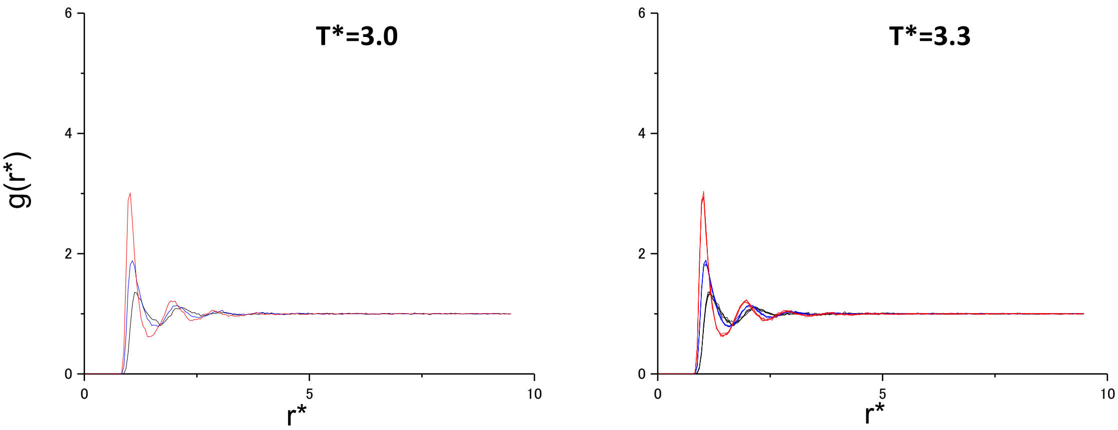

Figure S20. Radial distribution functions at the same temperatures of the snapshots of Figure S19 for the system ρ*= 0.56 and q* = 0.5 (black line) GB-GB RFD; (red line) LJ-LJ RDF; (blue line) GB-LJ RDF.

System ρ^* = 0.56

q^* = 5.0

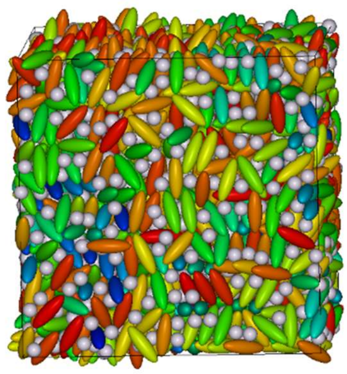

T*=0.6

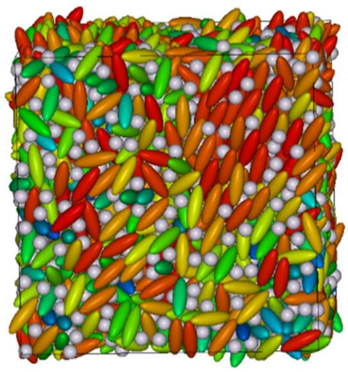

T*=1.0

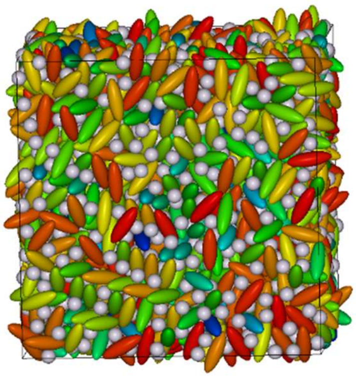

T*=1.2

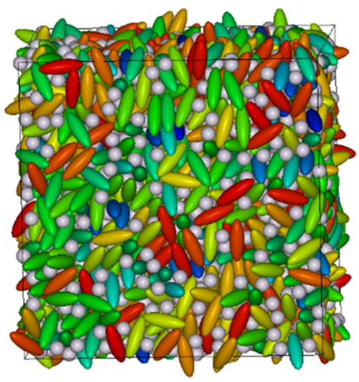

T*=1.4

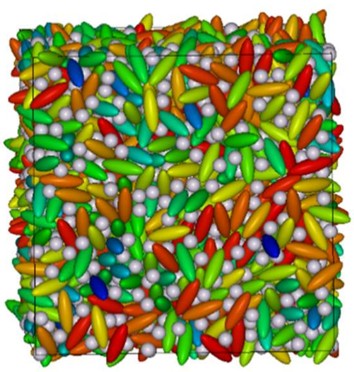

T*=1.6

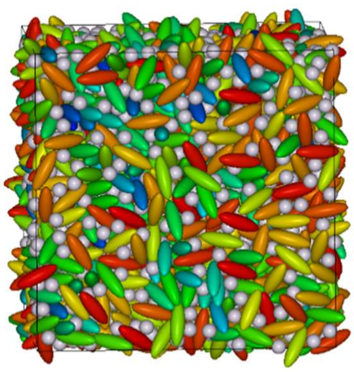

T*=1.8

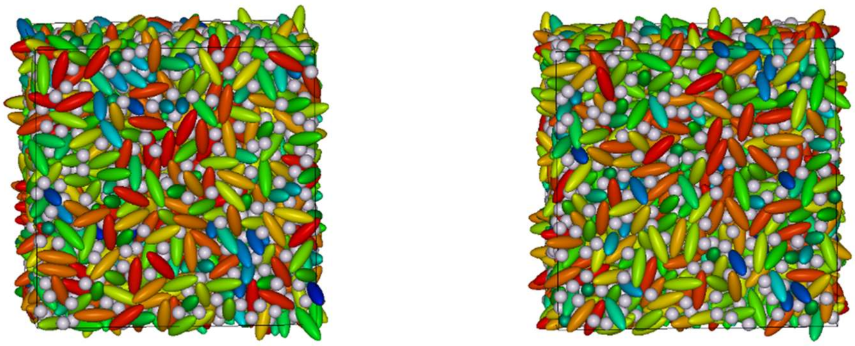

T*=2.0 **T*=2.4**

Figure S21. Snapshots obtained at the end of the production run for the system ρ^* = 0.56, q* = 5.0

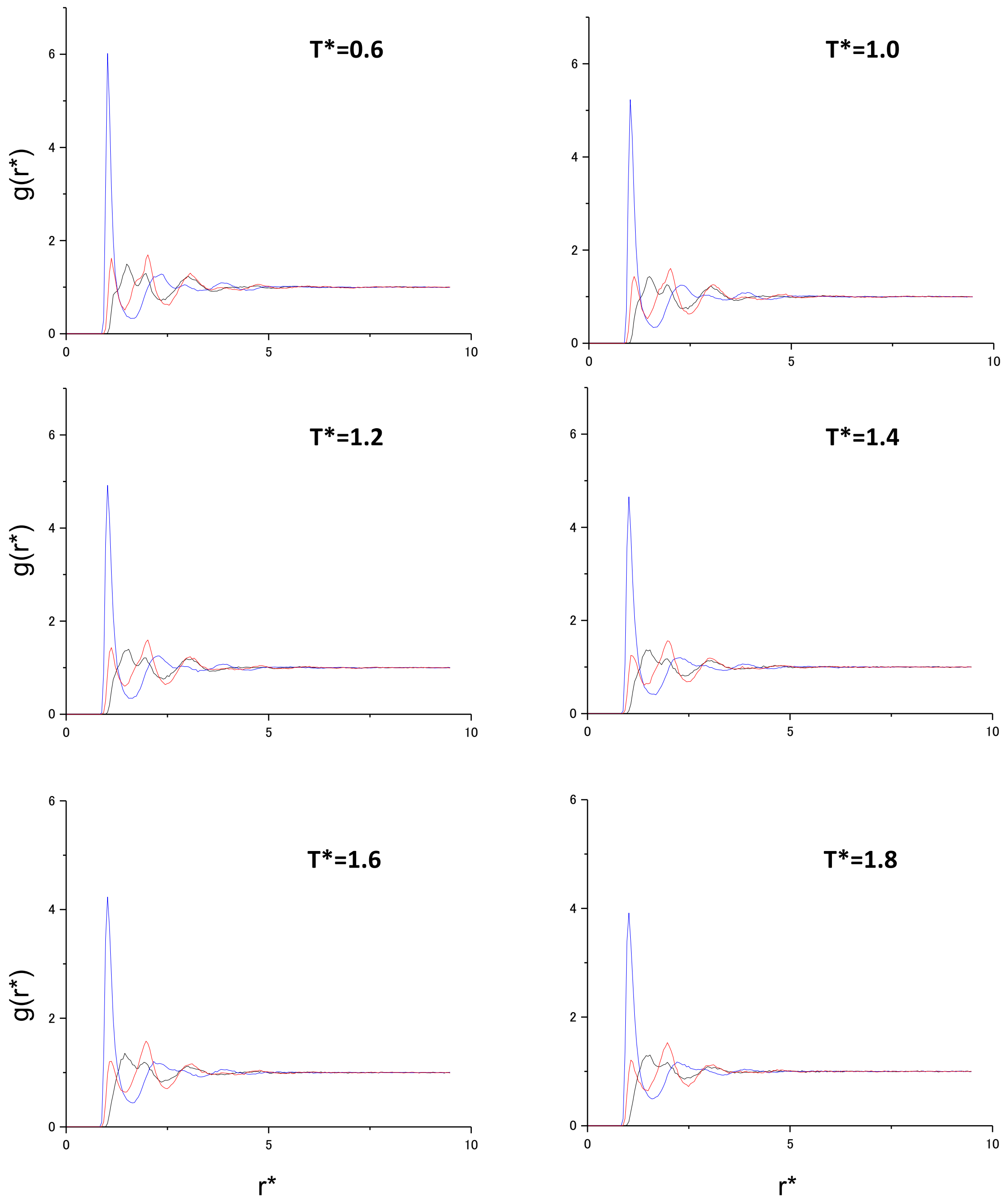
T*=0.6
T*=1.0
T*=1.2
T*=1.4
T*=1.6
T*=1.8
g(r*)
r*

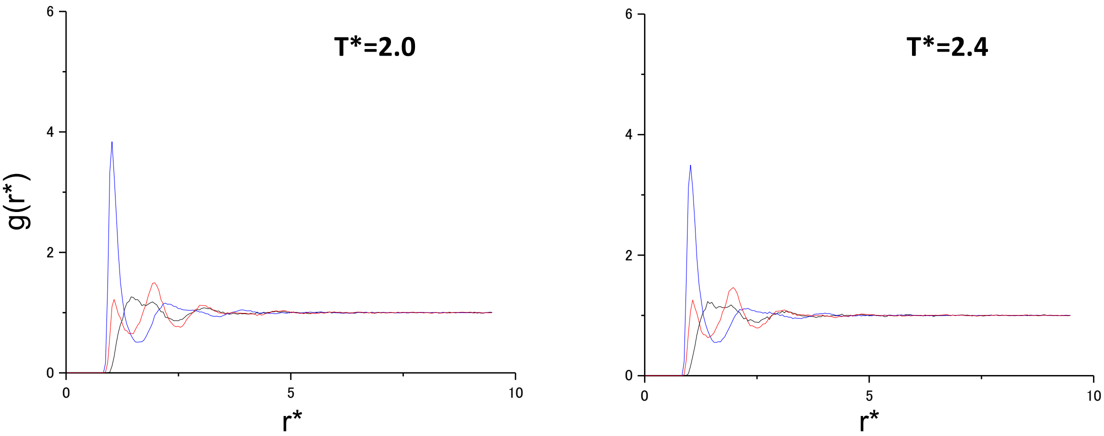

Figure S22. Radial distribution functions at the same temperatures of the snapshots of Figure S21 for the system ρ*= 0.56 and q* = 5.0 (black line) GB-GB RFD; (red line) LJ-LJ RDF; (blue line) GB-LJ RDF.

System ρ^* = 0.60

q^* = 0.0

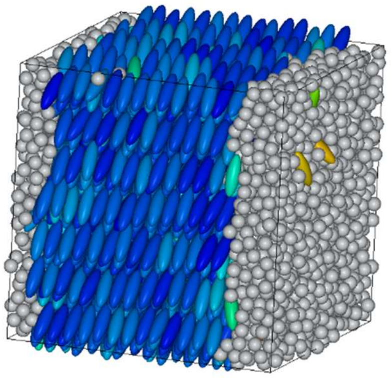

T*=2.5

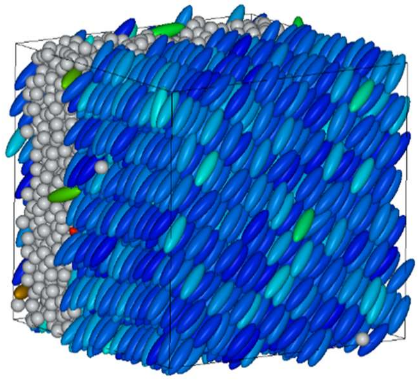

T*=2.6

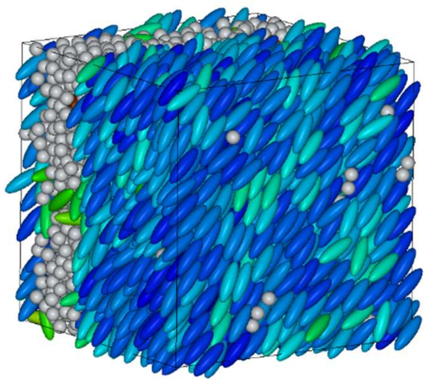

T*=2.7

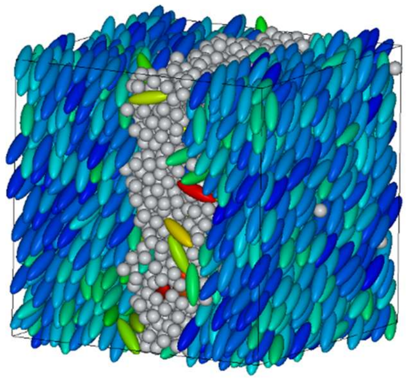

T*=2.8

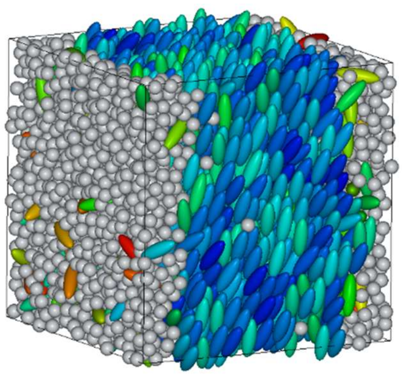

T*=2.9

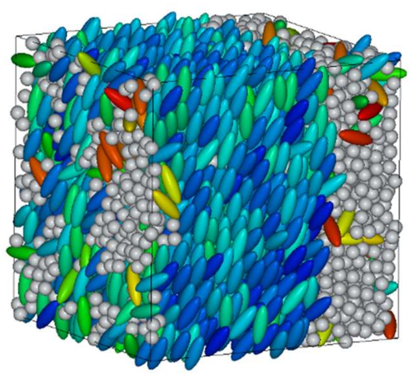

T*=3.0

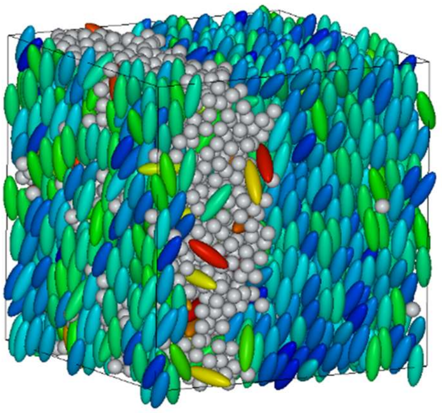

T*=3.1

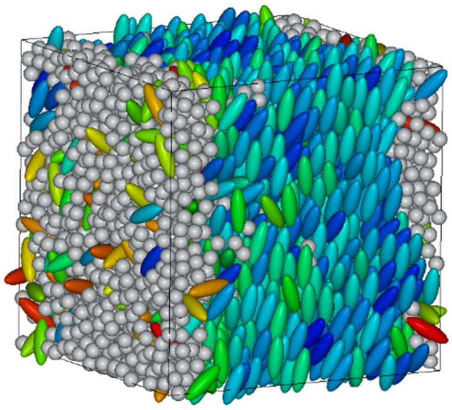

T*=3.2

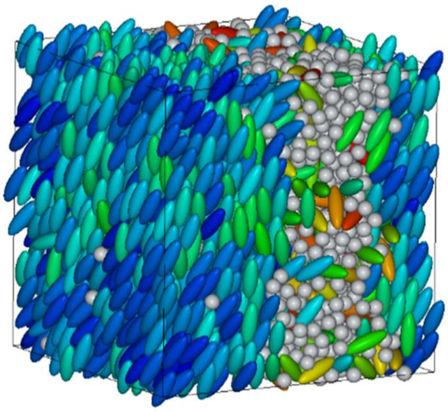

T*=3.3

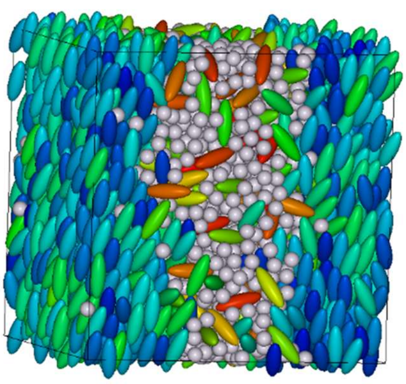

T*=3.4

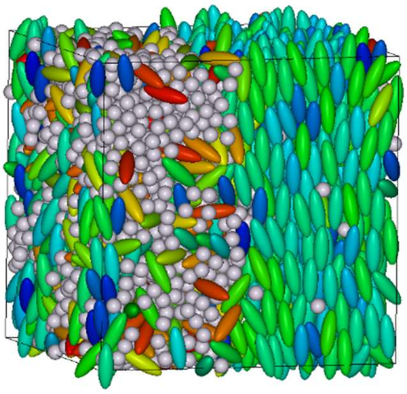

T*=3.5

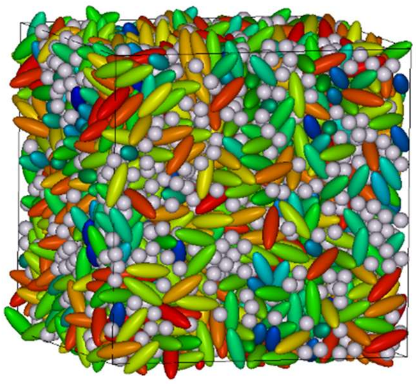

T*=3.6

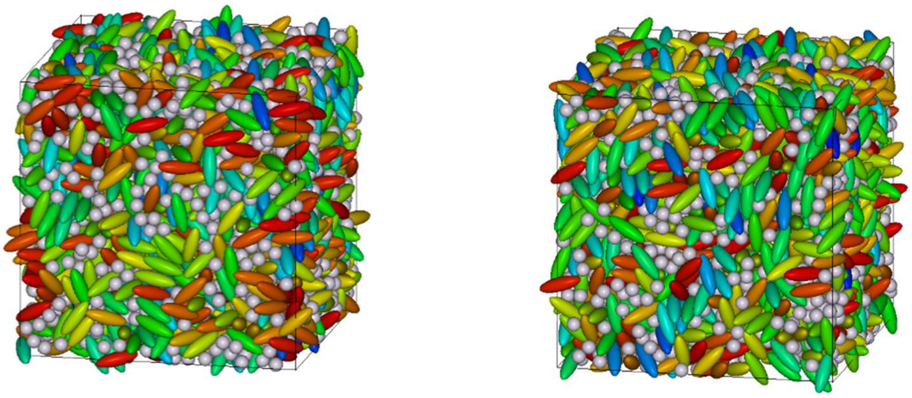

T*=3.7 T*=3.8

Figure S23. Snapshots obtained at the end of the production run for the system ρ^* = 0.60, q^* = 0.0

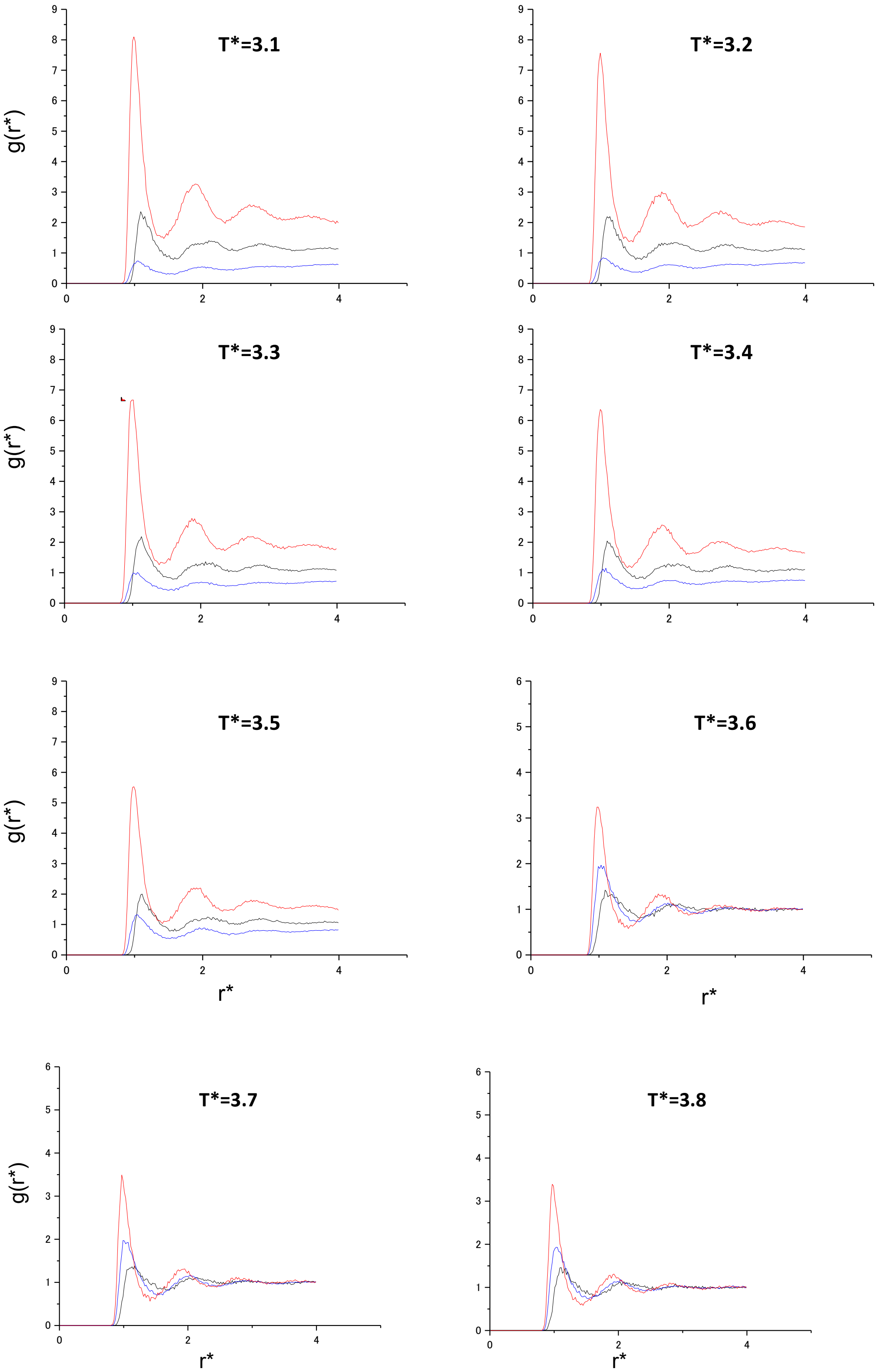

Figure S24. Radial distribution functions at the same temperatures of the snapshots of Figure S23 for the system ρ*= 0.60 and q* = 0.0 (black line) GB-GB RFD; (red line) LJ-LJ RDF; (blue line) GB-LJ RDF.

System ρ^* = 0.60

q^* = 0.5

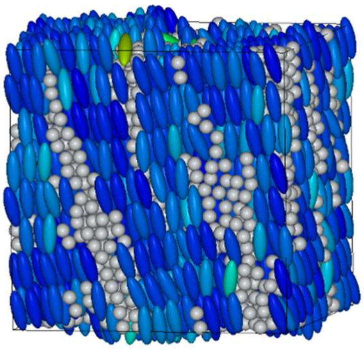

T*=2.0

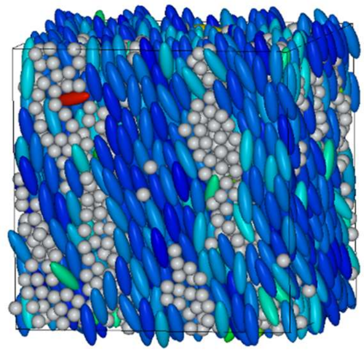

T*=2.1

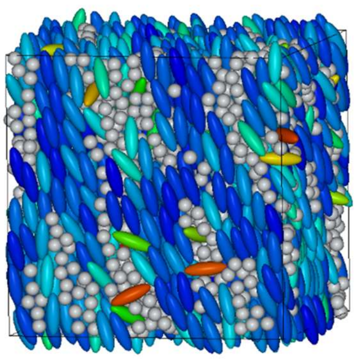

T*=2.2

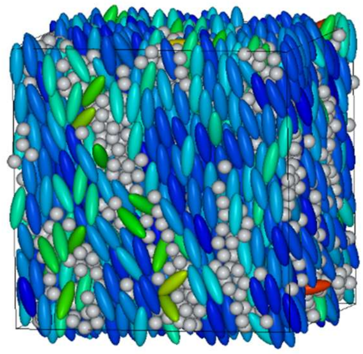

T*=2.3

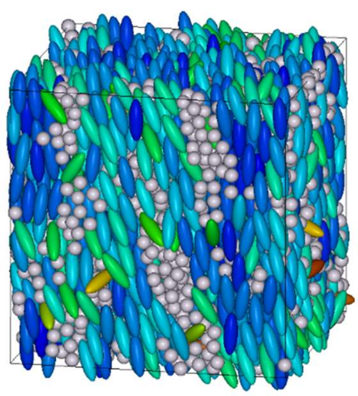

T*=2.4

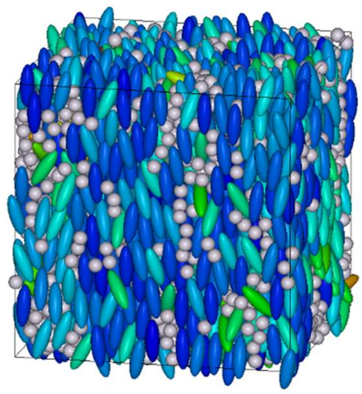

T*=2.5

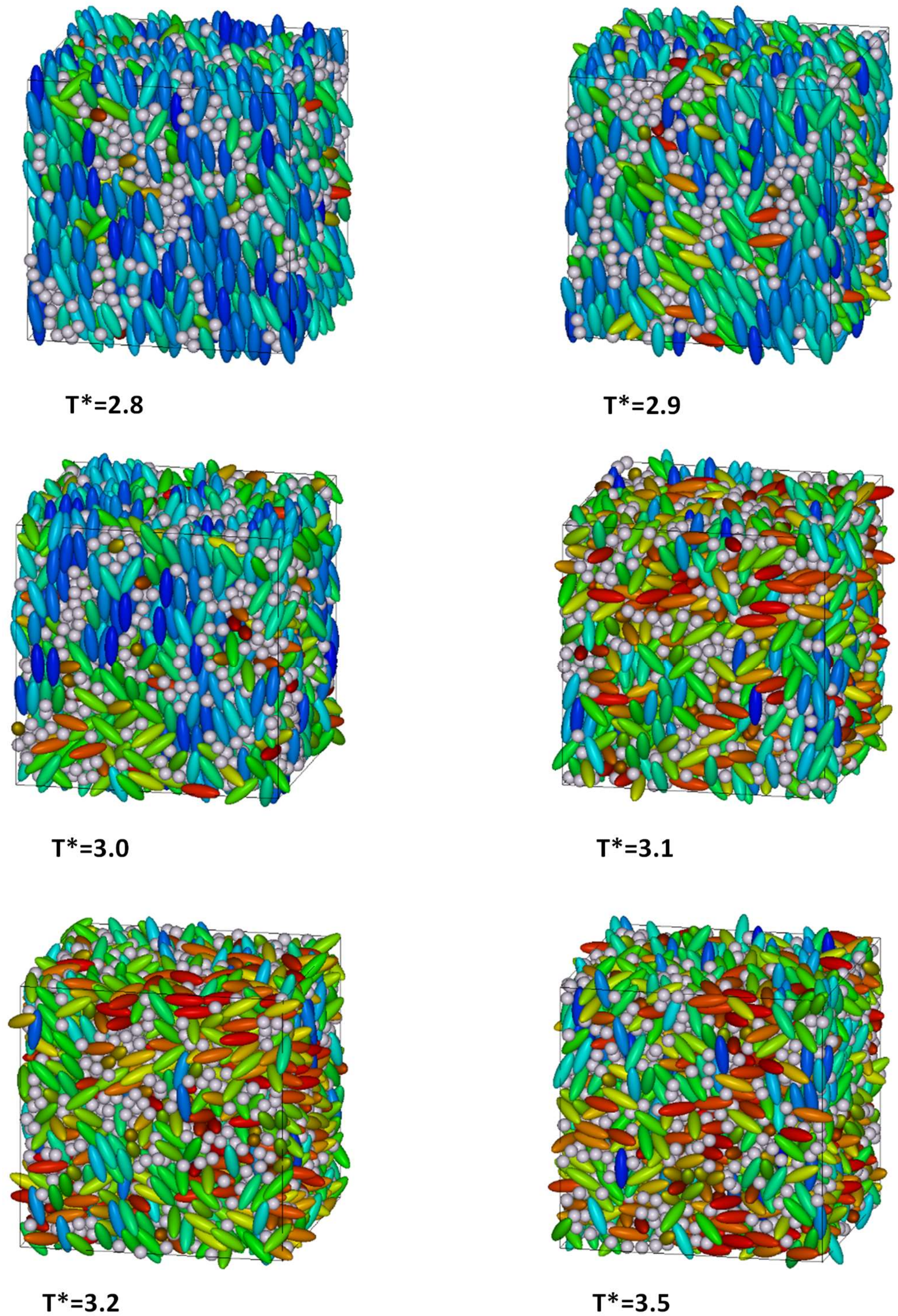

Figure S25. Snapshots obtained at the end of the production run for the system ρ* = 0.60, q* = 0.5

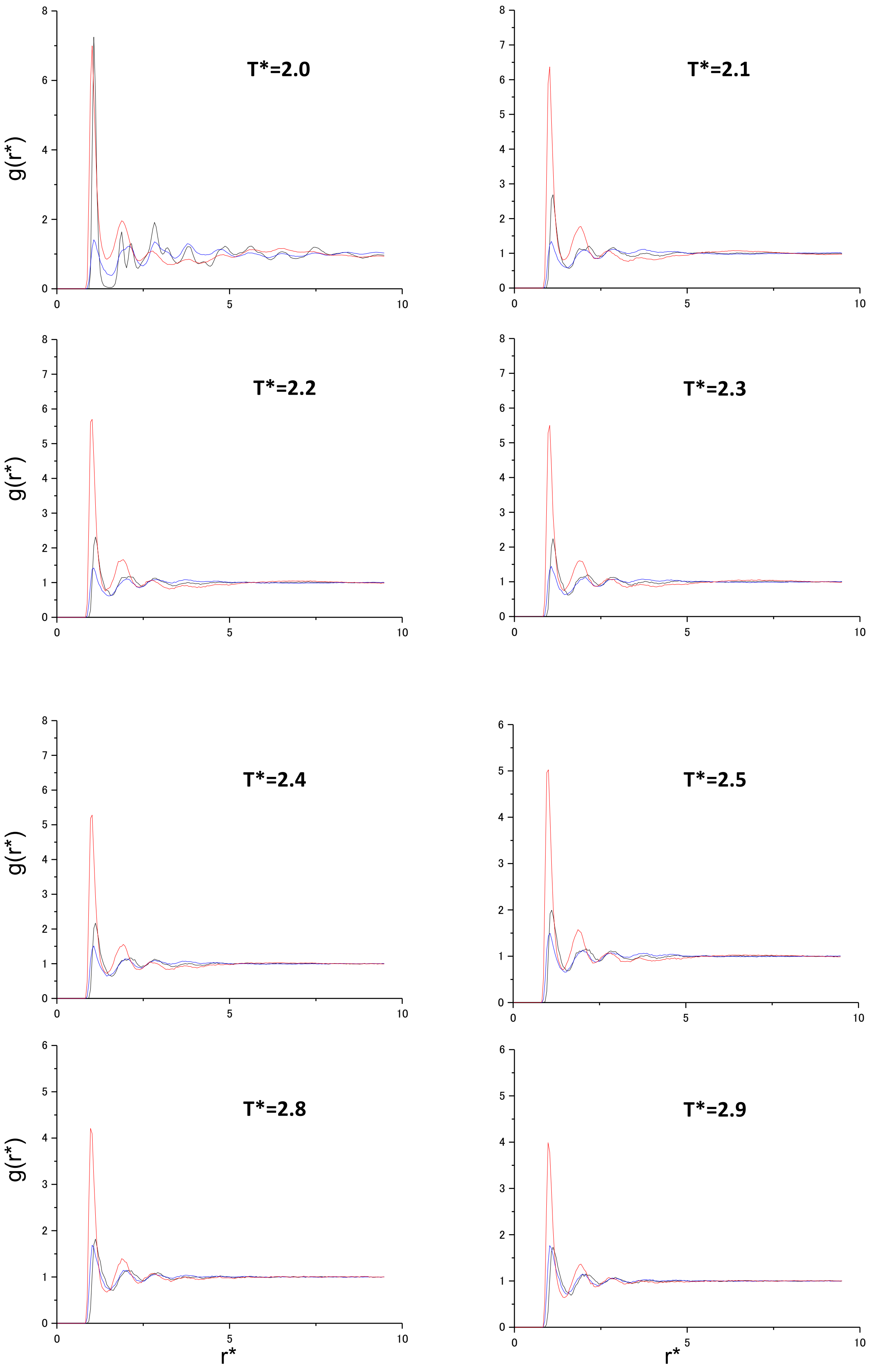
T*=2.0
T*=2.1
T*=2.2
T*=2.3
T*=2.4
T*=2.5
T*=2.8
T*=2.9
g(r*)
r*

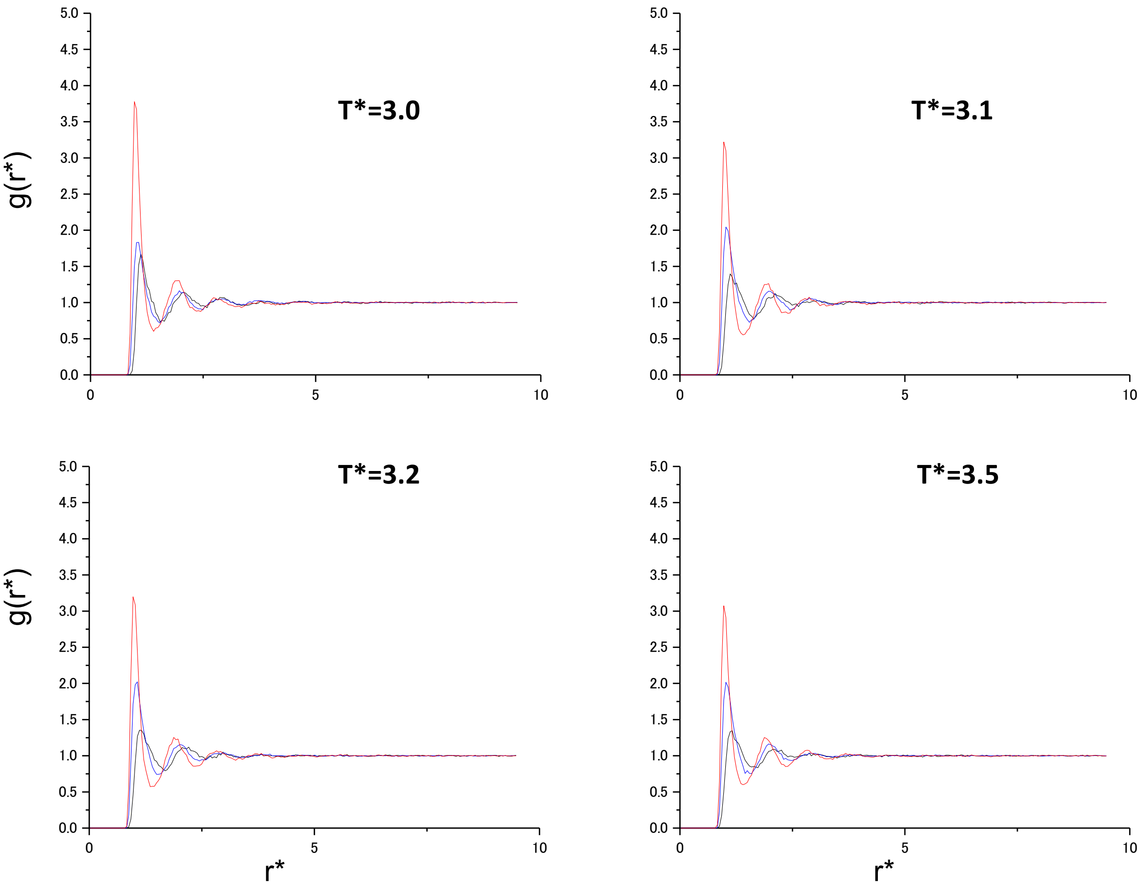

Figure S26. Radial distribution functions at the same temperatures of the snapshots of Figure S25 for the system ρ*= 0.60 and q* = 0.5 (black line) GB-GB RFD; (red line) LJ-LJ RDF; (blue line) GB-LJ RDF.

System ρ* = 0.60

q^* = 5.0

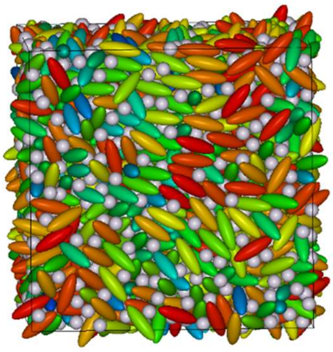

T*=1.0.

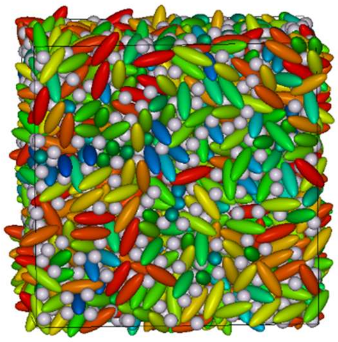

T*=1.5

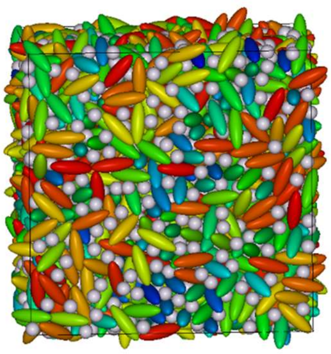

T*=2.1

Figure S27. Snapshots obtained at the end of the production run for the system ρ^* = 0.60, q^* = 5.0

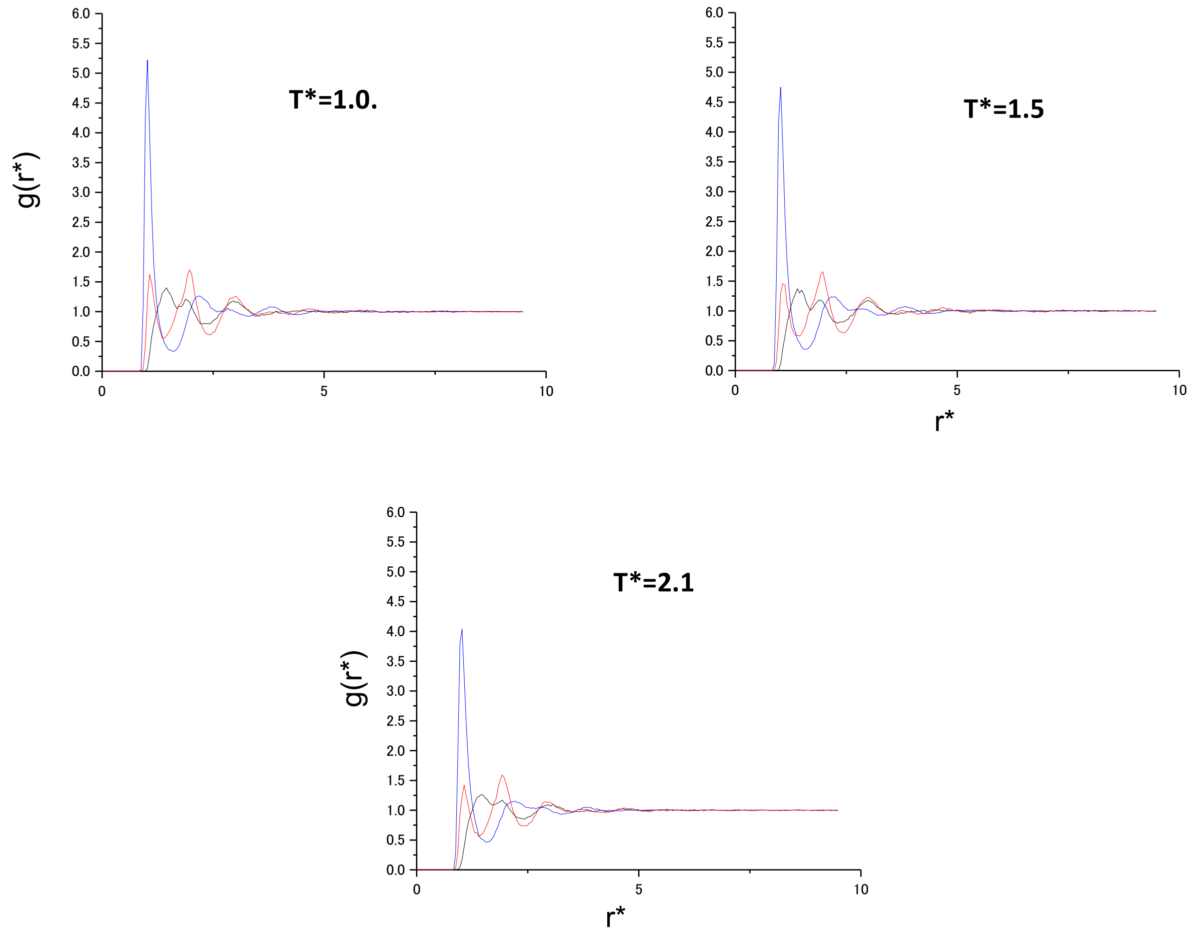

Figure S28. Radial distribution functions at the same temperatures of the snapshots of Figure S27 for the system ρ*= 0.60 and q* = 5.0 (black line) GB-GB RFD; (red line) LJ-LJ RDF; (blue line) GB-LJ RDF.

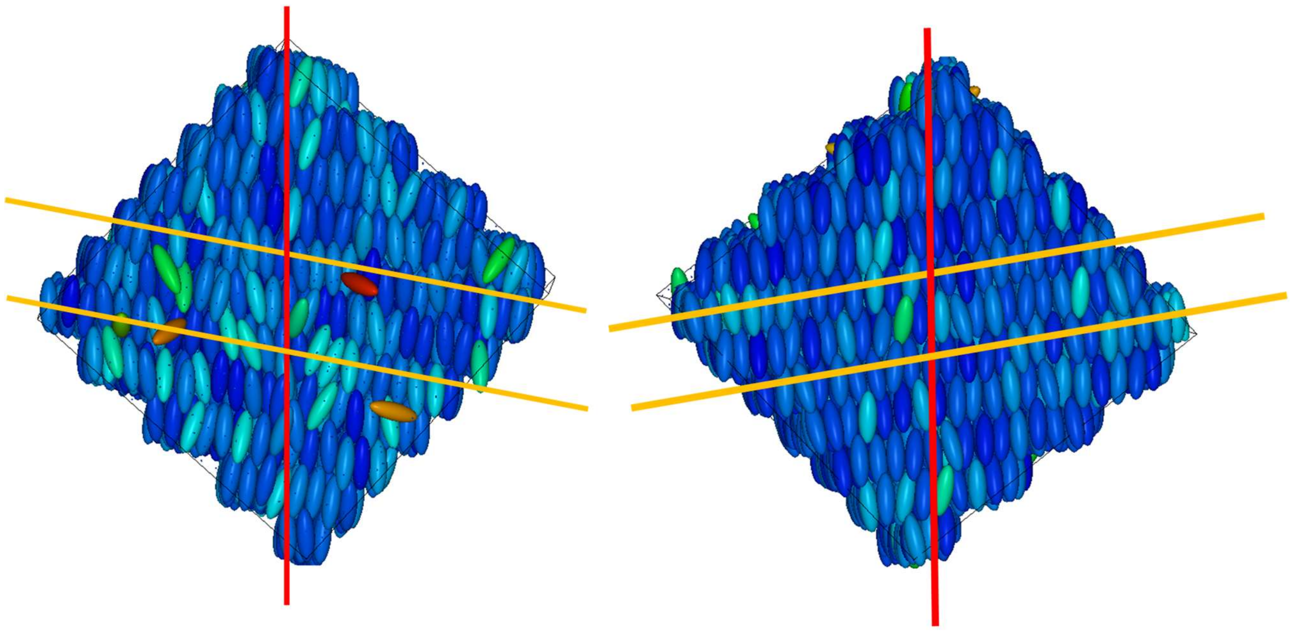

Figure S29. Snapshot of the systems ρ^* = 0.60, q^* = 0.0 at (left) T^* = 2.5 and (right) T^* = 2.6. Red line: director based on the average GB particle's orientation; Yellow line: some representative layers' orientation, to clearly highlight the tilt with the director.

Scaled units for van der Waals and Coulomb interaction

The values for the scaled parameters, m, ε_0 and σ_0 for the nematogen 4,4'-dimethoxyazoxybenzene (PAA) are m = 258 g mol^{-1}, ε_0 = 2.19 kJ mol^{-1}, σ_0=4.5 Å, respectively [R. Hashim, G. R. Luckhurst and S. Romano, *J. Chem. Soc. , Faraday Trans.,* 1995, **91**, 2141-2148].

This example is only intended as a proof that the scaled values used for all units are reasonable and not unphysical.

In SI Units, Coulomb's law is

$$V(r) = q_1 q_2/(4\pi\epsilon_0 r_{ij}) \text{ (Coulomb)}$$

where q_1 and q_2 are charges in Coulombs, and r_{ij} is their separation in meters, while the permittivity of the free space is ϵ_0 = 8.8542·10^{-12} C^{2}N^{-1}m^{-2}.

In reduced units based on the Lennard-Jones energy ε_0 and length σ_0 parameters, the charge is

$$q^* = q/(4\pi\epsilon_0\sigma_0\cdot\varepsilon_0)^{1/2}$$

Using the values of ε_0 and σ_0 mentioned above for a typical mesogen, when q = +1(e) (= 1.602·10^{-19} C), the dimensionless value of the scaled charge q^* is

$$q^* = q/(4\pi\epsilon_0\sigma_0\cdot\varepsilon_0)^{1/2} = 11.879$$

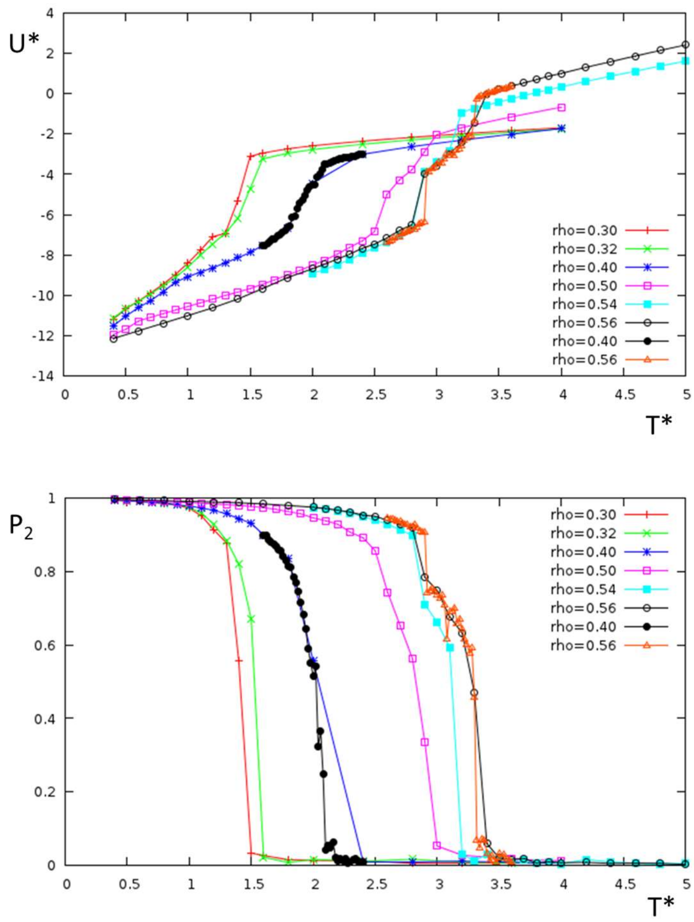

Figure S30 Results of some preliminary tests with a box of 1354 particles (677 GB and 677 LJ).

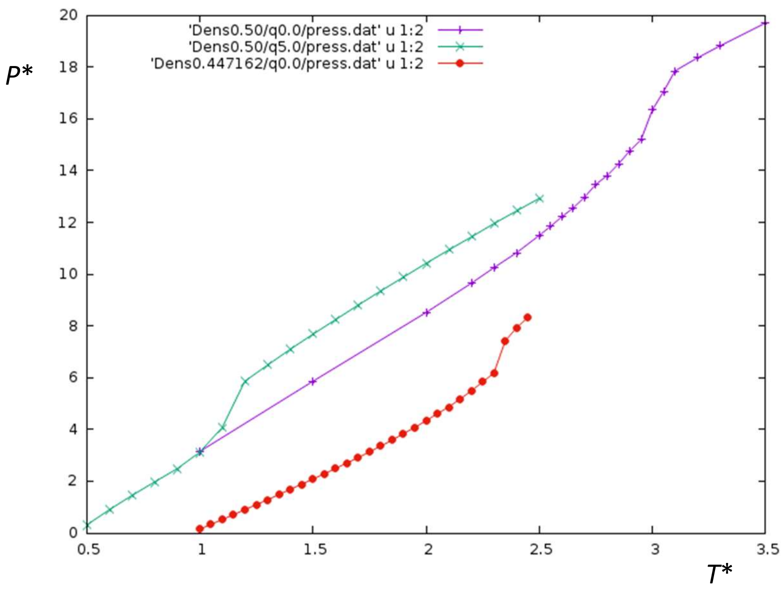

Figure S31 Dependence of the scaled pressure, P^*, on the scaled temperature, T^*, for some selected systems.

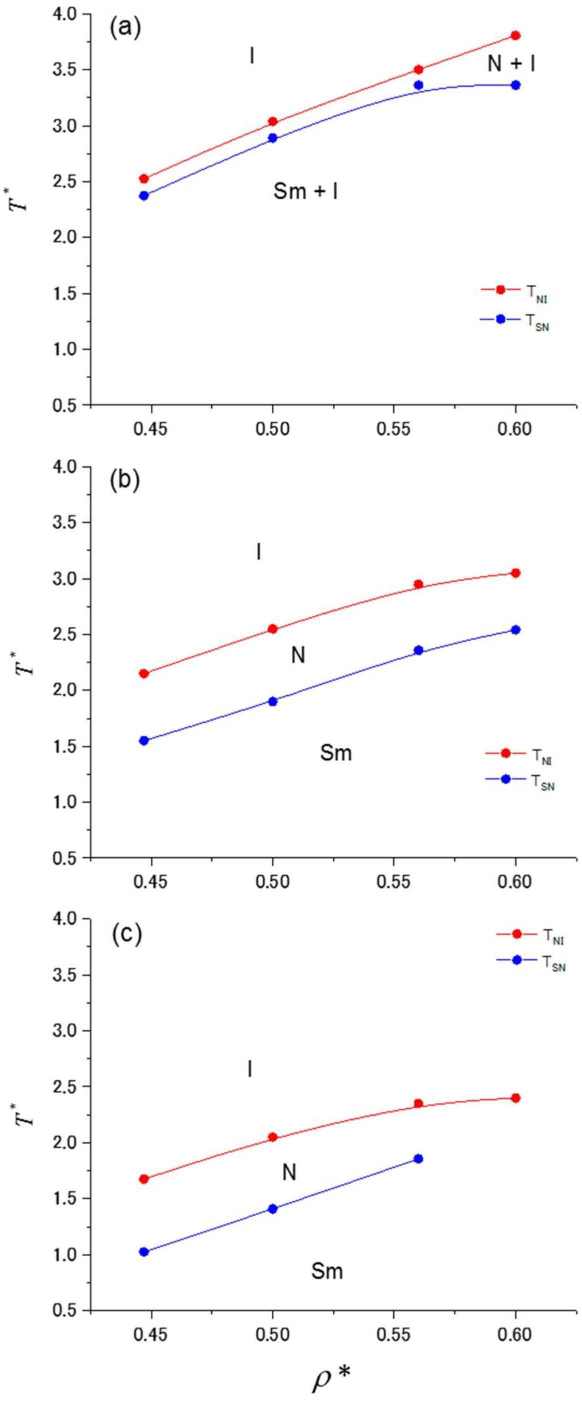

Figure S32 Phase diagrams for the systems with q^*=0.0 (a), 0.5 (b), 2.0 (c). The circles indicate transition temperatures evaluated from Eq.4) with cooling and heating data.

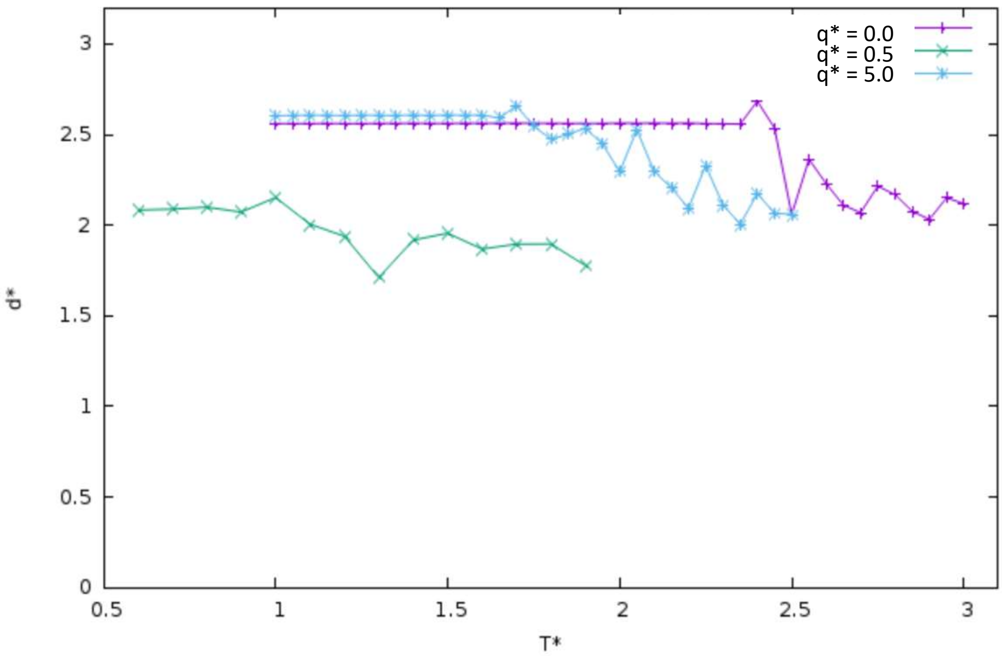

Figure S33 Example of the dependence of the parameter *d** maximizing Eq. 4) on the temperature for the systems with a density of 0.447.